Quantum Inf Process (2012) 11:269–309
DOI 10.1007/s11128-011-0242-1

Optimal conditions for Bell-inequality violation in the presence of decoherence and errors

A. G. Kofman

Received: 17 January 2011 / Accepted: 21 April 2011 / Published online: 21 May 2011

Abstract We obtain the set of all detector configurations providing the maximal violation of the Bell inequality in the Clauser–Horne–Shimony–Holt form for a general (pure or mixed) state of two qubits. Next, we analyze optimal conditions for the Bell-inequality violations in the presence of local decoherence, which includes energy relaxation at the zero temperature and arbitrary pure dephasing. We reveal that in most cases the Bell inequality violation is maximal for the "even" two-qubit state. Combined effects of measurement errors and decoherence on the Bell inequality violation are also discussed.

Keywords Bell's inequalities · Decoherence · Open quantum systems · Superconducting qubits

1 Introduction

Entanglement, i.e., quantum correlations between physical systems, is not only a basic feature of quantum behavior [21,50], but also an important resource for quantum computation and quantum information [42]. Decoherence, i.e., loss of coherence of states of quantum systems due to the interaction with the environment, is one of the major

A. G. Kofman (✉)
Department of Electrical Engineering, University of California, Riverside, CA 92521, USA
e-mail: kofmana@gmail.com

Present Address:
A. G. Kofman
Physics Department, The University of Michigan, Ann Arbor, MI 48109-1040, USA

A. G. Kofman
Advanced Science Institute, RIKEN, Wako-shi, Saitama 351-0198, Japan

stumbling blocks for quantum computation [42]. Therefore recently there has been a surge of interest in effects of decoherence on entanglement [9,29–31,33,35,48,52, 58,61,62]. In particular, it was revealed that, when decoherence is local (i.e., not correlated between different parts of a multipartite system), entanglement, as a rule, disappears after a finite time—the phenomenon called entanglement sudden death [61,62].

One of the most striking manifestations of the nonclassical nature of physics is violation of the Bell inequality (BI) [11]. In particular, the BI violations demonstrate non-locality of physics. Moreover, the BI violation is used for quantum key distribution [22,36]. Decoherence transforms a pure entangled state into a mixed state, decreasing thus entanglement and the Bell inequality violation. Effects of decoherence on the BI violation have attracted a significant interest recently [3,10,29–33,35,47,54]. Like entanglement, in the presence of local decoherence the BI violation in most cases disappears after a finite time (Bell nonlocality sudden death [3]).

A violation of the BI implies necessarily that the system is in an entangled state, however the converse statement is not true. Indeed, while any pure (completely coherent) entangled state can be used for violation of the BI [15,23], there are mixed (partially incoherent) entangled states which cannot violate the BI [60]. In fact, the ratio of the volume of the states violating the BI to the total volume of the entangled states is small; for instance, in the Hilbert–Schmidt metric this ratio equals 0.01085 [33]. Correspondingly, in the presence of local decoherence the duration of the Bell-inequality violation is generally significantly shorter than the entanglement survival time [33]. Thus, observation of the Bell inequality violation is a more difficult task than observation of entanglement.

Until now, most experiments on the BI violation have been performed with photons [2,5–8,59]. However, recently there has been an increasing interest in testing the BI for various material systems, where decoherence is usually an important factor. In particular, experiments with ions in traps [45], single neutrons [24], atom-photon [41] and two-atom [38] systems were performed. Moreover, the violation of the BI in superconducting Josephson phase qubits [13,17,37,63] was demonstrated in [4]. There are also various theoretical proposals related to the BI violation in solid-state systems [10,28,46,47,53,54,57].

Optimal experimental conditions for observation of the BI violation in superconducting phase qubits were considered in [32]. There both the ideal case and effects of various nonidealities, such as measurement errors and crosstalk [34,39], were analyzed in detail, while decoherence was discussed briefly. In a recent paper [33] entanglement and the BI violation in the presence of decoherence were considered. In both refs. [32,33], the class of the "odd" two-qubit states, which are obtained readily in experiments with superconducting phase qubits [39,51], was discussed. Note, however, that different states, such as "odd", "even" or more general states, are affected differently by energy relaxation. Therefore, it is of interest to study which states are better suited for observing violations of the BI in the presence of decoherence. Moreover, optimal detector configurations providing the maximal BI violation in the presence of decoherence were not discussed previously, except for the case of pure dephasing [47] (there are also brief remarks on this topics in [32,33]).

In the present paper, we consider the Bell inequality in the CHSH form [18] for two two-level systems (qubits). We begin with obtaining *all* optimal detector configurations providing the maximal BI violation for *any* given state. Basing on this solution, we provide a comprehensive discussion of effects of local decoherence on the BI violation. We obtain both optimal states and *all* detector configurations which yield the maximal BI violation in the presence of decoheremce. The knowledge of all optimal configurations is important for planning experiments, since some detector configurations can be easier to realize than others [47]. Our decoherence model includes energy relaxation at the zero temperature (known also as spontaneous decay or amplitude damping) and pure dephasing (phase damping). We analyze analytically and numerically the general case and a number of important special cases. In particular, we study the experimentally relevant classes of the general "even" and "odd" states and reveal that the "even" states provide maximal BI violations in most cases. We also discuss the combined effect of decoherence and local errors, basing on the treatment of errors in [32].

The paper is organized as follows. In Sect. 2 we discuss the BI and properties of maximally entangled states. In Sect. 3 we obtain all optimal configurations of the detectors which maximize the BI violation for any given (pure or mixed) state. Section 4 is devoted to effects of local (independent) decoherence of the qubits on the BI violation. In Sect. 5 we consider combined effects of errors and decoherence. Section 6 provides the concluding remarks. The two appendices supplement the main text. In particular, in Appendix B we discuss some properties of two-qubit states.

2 Preliminaries

2.1 The Bell inequality

We consider a pair of qubits, i.e., two-level systems a and b. Each qubit has the states $|0\rangle$ and $|1\rangle$. A measurement of a qubit along any direction in the Bloch-sphere produces one of possible results ± 1. The correlator of the measurement results for the two qubits is the following average (expected value),

$$E(\mathbf{a}, \mathbf{b}) = \langle A(\mathbf{a}) B(\mathbf{b}) \rangle. \tag{2.1}$$

Here $\mathbf{a}$ ($\mathbf{b}$) is the unit radius-vector in the Bloch sphere along the observation ("detector") axis for qubit a (b), whereas $A(\mathbf{a})$ and $B(\mathbf{b})$ are dichotomous random variables with the values ± 1 describing results of measurements for qubits a and b, respectively.

Measurements of two qubits satisfy the Bell inequality, provided that a local realistic (classical) theory holds and there is no communication between the qubits [11]. We consider the Clauser–Horne–Shimony–Holt (CHSH) version of the BI [12,18]

$$-2 \leq S \leq 2, \tag{2.2}$$

where

$$S = E(\mathbf{a}, \mathbf{b}) - E(\mathbf{a}, \mathbf{b}') + E(\mathbf{a}', \mathbf{b}) + E(\mathbf{a}', \mathbf{b}'). \tag{2.3}$$

Note that the minus sign can be moved to any term in Eq. (2.3). The resulting expressions for S are equivalent up to a change of the labeling of the observables at each qubit. Indeed, the substitution $\mathbf{a} \leftrightarrow \mathbf{a}'$ results in the permutation of the signs of the second and fourth terms in Eq. (2.3). Similarly, the substitution $\mathbf{b} \leftrightarrow \mathbf{b}'$ ($\mathbf{a} \leftrightarrow \mathbf{a}'$, $\mathbf{b} \leftrightarrow \mathbf{b}'$) is equivalent to moving the minus sign to the first (third) term in Eq. (2.3).

In the quantum case, the quantity (2.3) can be expressed through the Bell operator [14] $\mathscr{B}$ as follows,

$$S = \mathrm{Tr}\,(\mathscr{B}\rho), \tag{2.4}$$

where ρ is the density matrix for the two qubits and

$$\mathscr{B} = AB - AB' + A'B + A'B'. \tag{2.5}$$

Here the observables

$$A = \mathbf{a} \cdot \boldsymbol{\sigma}_a, \quad A' = \mathbf{a}' \cdot \boldsymbol{\sigma}_a, \quad B = \mathbf{b} \cdot \boldsymbol{\sigma}_b, \quad B' = \mathbf{b}' \cdot \boldsymbol{\sigma}_b, \tag{2.6}$$

where $\boldsymbol{\sigma}_a = \boldsymbol{\sigma} \otimes I_2$, $\boldsymbol{\sigma}_b = I_2 \otimes \boldsymbol{\sigma}$, I_n is the $n \times n$ identity matrix, and $\boldsymbol{\sigma} = (\sigma_x, \sigma_y, \sigma_z)$ is the vector of the Pauli matrices [42]. We denote by $|0\rangle$ and $|1\rangle$ the eigenvectors of σ_z with the eigenvalues 1 and -1, respectively.[1]

The CHSH parameter S depends on the quantum state of the pair of qubits and on the "detector configuration", i.e., the four vectors $(\mathbf{a}, \mathbf{a}', \mathbf{b}, \mathbf{b}')$. In this paper we look for experimental conditions, i.e., the quantum states and the corresponding detector configurations, which are the most favorable for an observation of the BI violation. Such conditions are reached when $|S| - 2$ is positive and maximal.

We will use the following properties of S [32].

(i) S is invariant under arbitrary local unitary transformations of the qubits,

$$\rho \to (U_a \otimes U_b)\rho(U_a^\dagger \otimes U_b^\dagger), \tag{2.7a}$$

and the corresponding rotations of the detectors,

$$\mathbf{a} \to \mathsf{R}_a\mathbf{a}, \quad \mathbf{a}' \to \mathsf{R}_a\mathbf{a}', \quad \mathbf{b} \to \mathsf{R}_b\mathbf{b}, \quad \mathbf{b}' \to \mathsf{R}_b\mathbf{b}'. \tag{2.7b}$$

Here U_a (U_b) is a unitary matrix for qubit a (b) and R_a (R_b) is the rotation matrix corresponding to U_a (U_b), so that, e.g.,

$$U_a(\mathbf{r}_a \cdot \boldsymbol{\sigma})U_a^\dagger = (\mathsf{R}_a\mathbf{r}_a) \cdot \boldsymbol{\sigma}, \tag{2.8}$$

[1] The present notation for the qubit states differs from that used in [32,33] by the permutation of the states $|0\rangle$ and $|1\rangle$.

a rotation matrix R being an orthogonal matrix, $\mathsf{R}^T\mathsf{R} = I_3$, with $\det(\mathsf{R}) = 1$. Equation (2.7b) is obtained on inserting Eq. (2.7a) into Eq. (2.4) and using Eqs. (2.5), (2.6), and (2.8).

(ii) The sign of S is inverted, if the vectors $\mathbf{a}$ and $\mathbf{a}'$ (or $\mathbf{b}$ and $\mathbf{b}'$) invert the sign,

$$S \to -S \quad \text{if} \;\; \mathbf{a} \to -\mathbf{a},\;\; \mathbf{a}' \to -\mathbf{a}' \;\; \text{or} \;\; \mathbf{b} \to -\mathbf{b},\;\; \mathbf{b}' \to -\mathbf{b}'. \tag{2.9}$$

Therefore, for a given state the maximal and minimal values of S are equal by the magnitude, yielding equal violations of both bounds in the BI (2.2). In other words,

$$S_+ = -S_-, \tag{2.10}$$

where S_+ and S_- are, respectively, the maximum and minimum of S for a given state. As a result, it is sufficient to discuss only the conditions for achieving the maximum of S, at least, in the absence of the measurements errors (effects of errors are discussed in Sect. 5). Below we denote by $S_{\max}$ the maximum of $|S|$ over all states and detector axes.

(iii) Equation (2.9) implies that S is not changed if all detectors are inverted,

$$(\mathbf{a}, \mathbf{a}', \mathbf{b}, \mathbf{b}') \to (-\mathbf{a}, -\mathbf{a}', -\mathbf{b}, -\mathbf{b}'). \tag{2.11}$$

2.2 Maximally entangled states

In the ideal case, when there is no decoherence or errors, the maximal and minimal values, $S_{\max}$ and $S_{\min}$, which S can achieve are [16]

$$S_{\max} = 2\sqrt{2}, \quad S_{\min} = -2\sqrt{2}. \tag{2.12}$$

These limits are obtained for any maximally entangled state [44]. The BI violations are often considered for the following maximally entangled states, called also the Bell states [42],

$$|\Phi_\pm\rangle = (|00\rangle \pm |11\rangle)/\sqrt{2}, \tag{2.13}$$
$$|\Psi_\pm\rangle = (|01\rangle \pm |10\rangle)/\sqrt{2}. \tag{2.14}$$

For each maximally entangled state there are infinitely many optimal (i.e., producing a maximal BI violation) configurations of the detector axes $\mathbf{a}$, $\mathbf{a}'$, $\mathbf{b}$, and $\mathbf{b}'$; all such configurations were described in [32]. In Sect. 3 we describe all configurations maximizing S for an arbitrary (pure or mixed) state.

It is useful to have a general expression for maximally entangled states in the "standard" basis of the qubit pair. As shown in Sect. 2.3, with the accuracy to an overall phase, the most general form of a maximally entangled state is[2]

$$|\Psi\rangle = c_1|00\rangle + c_2 e^{i\alpha_a}|01\rangle - c_2 e^{i\alpha_b}|10\rangle + c_1 e^{i(\alpha_a+\alpha_b)}|11\rangle \tag{2.15}$$

[2] An expression equivalent to Eq. (2.15), but written in a different basis, was cited in [56].

Here α_a, α_b, c_1, and c_2 are real numbers, and $c_1^2 + c_2^2 = 1/2$.

With the help of local rotations of the qubits around the z axis, the coefficients in Eq. (2.15) can be made real, yielding one of the two states

$$|\Psi\rangle = c_\Phi|\Phi_\pm\rangle + c_\Psi|\Psi_\mp\rangle, \tag{2.16}$$

where either the upper or the lower signs should be used simultaneously, c_Φ and c_Ψ are any real numbers satisfying $c_\Phi^2 + c_\Psi^2 = 1$, and $|\Phi_\pm\rangle$ and $|\Psi_\pm\rangle$ are the Bell states (2.13) and (2.14). Equations (2.15) and (2.16) are used in Sect. 4.

2.3 BI violations and entanglement for pure states

In the presence of decoherence and/or measurement errors, the states providing the maximal BI violation are not necessarily the maximally entangled states. Here we discuss the BI violations for arbitrary pure states under ideal conditions, i.e., in the absence of decoherence and errors.

There is a relation [55] (see also Appendix A) between S_+ and an entanglement measure, the concurrence $\mathscr{C}$ [25], for an arbitrary two-qubit pure state,

$$S_+ = 2\sqrt{1 + \mathscr{C}^2}. \tag{2.17}$$

The concurrence $\mathscr{C}$ is limited by the condition $0 \le \mathscr{C} \le 1$, a state being entangled whenever $\mathscr{C} > 0$. Equation (2.17) shows that the BI is always violated for an entangled pure state, the maximal violation S_+ increasing with the concurrence $\mathscr{C}$.

Let us obtain S_+ and $\mathscr{C}$ for an arbitrary two-qubit pure state, which, up to an overall phase, can be written in the form

$$|\Psi\rangle = c_1|00\rangle + c_2 e^{i\alpha_b}|01\rangle + c_3 e^{i\alpha_a}|10\rangle + c_4 e^{i(\alpha_a+\alpha_b+\alpha)}|11\rangle, \tag{2.18}$$

where α_a, α_b, α, and c_i are real numbers, and $\sum_{i=1}^4 c_i^2 = 1$. Since S_+ is invariant with respect to local qubit rotations [the property (i) in Sect. 2.1], the state (2.18) has the same value of S_+ as the state

$$|\Psi\rangle = c_1|00\rangle + c_2|01\rangle + c_3|10\rangle + c_4 e^{i\alpha}|11\rangle, \tag{2.19}$$

obtained from Eq. (2.18) by rotating the qubits a and b around the z axis by the angles $-\alpha_a$ and $-\alpha_b$, respectively.

As shown in Appendix A, for the state (2.18)

$$\mathscr{C} = 2|c_1 c_4 e^{i\alpha} - c_2 c_3|. \tag{2.20}$$

This result provides also S_+ by Eq. (2.17). Equation (2.20) implies that for given probabilities c_i^2, the concurrence and BI violation are maximized in the state (2.18), when

$$\alpha = 0, \quad c_1 c_2 c_3 c_4 < 0. \tag{2.21}$$

Then Eqs. (2.18) and (2.19) become

$$|\Psi\rangle = c_1|00\rangle + c_2 e^{i\alpha_b}|01\rangle + c_3 e^{i\alpha_a}|10\rangle + c_4 e^{i(\alpha_a+\alpha_b)}|11\rangle, \tag{2.22}$$

and

$$|\Psi\rangle = c_1|00\rangle + c_2|01\rangle + c_3|10\rangle + c_4|11\rangle, \tag{2.23}$$

whereas the concurrence (2.20) in Eqs. (2.22) and (2.23) becomes

$$\mathscr{C} = 2(|c_1c_4| + |c_2c_3|). \tag{2.24}$$

The condition (2.21) can hold only when all $c_i \neq 0$. Otherwise, when, at least, one of the amplitudes c_i vanishes, the concurrence (2.20) is independent of α, being given by Eq. (2.24), where now at most one term is nonzero. In this case the general state (2.18) is equivalent to the real state (2.23) up to local z-rotations of the qubits.

Let us maximize $\mathscr{C}$ (2.24) and hence S_+. We proceed in two stages. First, we keep c_2 and c_3 fixed and vary c_1 and c_4 under the condition that $c_1^2 + c_4^2 = 1 - c_2^2 - c_3^2$ is fixed. This provides the maximization condition $|c_1| = |c_4|$. Similarly, varying c_2 and c_3 with $|c_1| = |c_4|$ being fixed yields the maximization condition $|c_2| = |c_3|$. Under the above two conditions, $\mathscr{C} = 1$ and $S_+ = 2\sqrt{2}$, i.e., the state is maximally entangled. We should also satisfy the inequality in Eq. (2.21) whenever $c_1 \neq 0$ and $c_2 \neq 0$. This is achieved by setting $c_4 = c_1$ and $c_3 = -c_2$ in Eq. (2.22); as a result, we obtain the general expression (2.15) for maximally entangled states.

In summary, we have shown that for given probabilities c_i^2, the BI violation and entanglement are maximized in real states (2.23) as well as in states which are equivalent to real states up to local z-rotations of the qubits.

3 Conditions for the maximal BI violation in an arbitrary state

While the formula for the maximum S_+ of S in the general mixed state is known [27], only one optimal detector configuration (i.e., a configuration for which S_+ is realized) was provided [27,23,43]. In contrast, Samuelsson et al. [47] showed that for the Bell state $|\Phi_+\rangle$ in the presence of dephasing there is a family of optimal configurations depending on one continuous parameter. In this section we extend the method of [27] in order to obtain all optimal detector configurations for any (pure or mixed) state. We show that the set of optimal detector configurations generally depends on one continuous and one discrete parameters, though in special cases the number of continuous parameters can equal two or three.

3.1 Maximal BI violation

Let us review the derivation [27] of the maximum S_+ of S for a given state. It is useful to consider the following representation [26,27,49] of the two-qubit density matrix

$$\rho = \left(I_4 + \mathbf{r}_a \cdot \boldsymbol{\sigma}_a + \mathbf{r}_b \cdot \boldsymbol{\sigma}_b + \boldsymbol{\sigma}_a \mathsf{T} \boldsymbol{\sigma}_b\right)/4. \tag{3.1}$$

Here $\mathbf{r}_k$ is the Bloch vector characterizing the reduced density matrix for the qubit k, so that, e.g., $\rho_a = \mathrm{Tr}_b \rho = (I_2 + \mathbf{r}_a \cdot \boldsymbol{\sigma})/2$, T is a matrix with the real elements

$$\mathsf{T}_{mn} = \mathrm{Tr}\,(\rho \sigma_m^a \sigma_n^b) \quad (m, n = x, y, z), \tag{3.2}$$

and $\boldsymbol{\sigma}_a \mathsf{T} \boldsymbol{\sigma}_b = \sum_{m,n=x}^{z} \mathsf{T}_{mn} \sigma_m^a \sigma_n^b$, where $\boldsymbol{\sigma}_k = (\sigma_x^k, \sigma_y^k, \sigma_z^k)$ $(k = a, b)$. Some useful properties of T are discussed in Appendix B.

Inserting Eq. (2.5) into (2.4) and taking into account Eqs. (2.6) and (3.2), we obtain that

$$S = \mathbf{a}\mathsf{T}\mathbf{b} - \mathbf{a}\mathsf{T}\mathbf{b}' + \mathbf{a}'\mathsf{T}\mathbf{b} + \mathbf{a}'\mathsf{T}\mathbf{b}'. \tag{3.3}$$

The products of the form $\mathbf{a}\mathsf{T}\mathbf{b}$ in Eq. (3.3) and below are defined as follows,

$$\mathbf{a}\mathsf{T}\mathbf{b} = \mathbf{a} \cdot (\mathsf{T}\mathbf{b}) = \sum_{m,n=x}^{z} \mathsf{T}_{mn} a_m b_n. \tag{3.4}$$

The vectors $\mathbf{b}$ and $\mathbf{b}'$ can be always written in the form [43]

$$\begin{aligned} \mathbf{b} &= \mathbf{c}_1' \cos(\zeta_b/2) + \mathbf{c}_2' \sin(\zeta_b/2), \\ \mathbf{b}' &= \mathbf{c}_1' \cos(\zeta_b/2) - \mathbf{c}_2' \sin(\zeta_b/2), \end{aligned} \tag{3.5}$$

where $\mathbf{c}_1'$ and $\mathbf{c}_2'$ are orthogonal unit vectors and ζ_b is the angle between $\mathbf{b}$ and $\mathbf{b}'$ $(0 < \zeta_b < \pi)$. Inserting Eq. (3.5) into (3.3) yields $S = 2[\mathbf{a}\mathsf{T}\mathbf{c}_2' \sin(\zeta_b/2) + \mathbf{a}'\mathsf{T}\mathbf{c}_1' \cos(\zeta_b/2)]$. To maximize this expression, one should require $\mathbf{a}$ and $\mathbf{a}'$ to be parallel to $\mathsf{T}\mathbf{c}_2'$ and $\mathsf{T}\mathbf{c}_1'$, respectively,[3] yielding

$$\mathbf{a} = \frac{\mathsf{T}\mathbf{c}_2'}{|\mathsf{T}\mathbf{c}_2'|}, \quad \mathbf{a}' = \frac{\mathsf{T}\mathbf{c}_1'}{|\mathsf{T}\mathbf{c}_1'|}. \tag{3.6}$$

Then maximizing S over ζ_b results in

$$\zeta_b = 2 \arctan\left(\frac{|\mathsf{T}\mathbf{c}_2'|}{|\mathsf{T}\mathbf{c}_1'|}\right), \tag{3.7}$$

[3] Here the symbols $\mathbf{a}$ and $\mathbf{a}'$ are interchanged in comparison with [27] in view of the difference of the definitions of S in the present paper and in [27] (cf. the last paragraph in Sect. 2.1).

where $|\mathbf{v}|$ denotes the length of a vector $\mathbf{v}$, and

$$S = 2\sqrt{|\mathsf{T}\mathbf{c}_1'|^2 + |\mathsf{T}\mathbf{c}_2'|^2} = 2\sqrt{\mathbf{c}_1'\mathsf{U}\,\mathbf{c}_1' + \mathbf{c}_2'\mathsf{U}\,\mathbf{c}_2'}. \tag{3.8}$$

Here

$$\mathsf{U} = \mathsf{T}^T\mathsf{T} \tag{3.9}$$

is a real symmetric matrix with nonnegative eigenvalues $u_1,\ u_2, u_3$; u_3 being the smallest eigenvalue ($0 \leq u_3 \leq u_1, u_2$). As shown in [27],

$$\max_{\mathbf{c}_1',\mathbf{c}_2'}(\mathbf{c}_1'\mathsf{U}\,\mathbf{c}_1' + \mathbf{c}_2'\mathsf{U}\,\mathbf{c}_2') = u_1 + u_2 \tag{3.10}$$

(see the proof in Sect. 3.2). Equations (3.8) and (3.10) yield the maximum of S [27],

$$S_+ = 2\sqrt{u_1 + u_2}. \tag{3.11}$$

Hence, the BI violation, $S_+ > 2$, occurs when $u_1 + u_2 > 1$. Equations (B.4) and (3.11) imply the following limits on S_+,

$$0 \leq S_+ \leq 2\sqrt{2}. \tag{3.12}$$

In particular, for pure states [23] $2 \leq S_+ \leq 2\sqrt{2}$. The lower limit in Eq. (3.12), $S_+ = 0$, is obtained for the states with $\mathsf{T} = 0$, which are, in view of Eq. (B.6), the states locally equivalent to $\rho = \mathrm{diag}(\rho_{11}, \rho_{22}, 1/2 - \rho_{22}, 1/2 - \rho_{11})$. These states are product states with one of the qubits in the maximally mixed state $I_2/2$ and mixtures of such states.

As an example, let us obtain S_+ for a state with a diagonal T. As shown in Appendix B, all such states have the form (B.5). Now $\mathsf{U} = \mathsf{T}^2$, and Eqs. (B.6) and (3.11) imply that

$$S_+ = 2[\max\{8\rho_{23}^2 + 8\rho_{14}^2, 4(|\rho_{23}| - |\rho_{14}|)^2 + (1 - 2\rho_{22} - 2\rho_{33})^2\}]^{1/2}. \tag{3.13}$$

As shown in Appendix B, a necessary condition for the BI violation is $\det(\mathsf{T}) < 0$, which implies that

$$\mathsf{T} = -\mathsf{R}\sqrt{\mathsf{U}}, \tag{3.14}$$

where $\mathsf{R} = -\mathsf{T}\mathsf{U}^{-1/2}$ is a rotation matrix. Below we focus on the case $\det(\mathsf{T}) < 0$.

3.2 Optimal detector configurations

Consider detector configurations providing the maximal S (3.11). Equation (3.10) obviously holds for $\mathbf{c}_1' = \mathbf{c}_1$ and $\mathbf{c}_2' = \mathbf{c}_2$, where $\mathbf{c}_i$ ($i = 1, 2, 3$) are the unit orthogonal eigenvectors of U corresponding to the eigenvalues u_i. This is the choice of $\mathbf{c}_1'$

and $\mathbf{c}_2'$ which was made in [27] (similar choices were made also in [23] and [43]). In this case Eq. (3.7) becomes $\zeta_b = \zeta_0$, where

$$\zeta_0 = 2\arctan\sqrt{\frac{u_2}{u_1}}, \tag{3.15}$$

since $|\mathsf{T}\mathbf{c}_i|^2 = \mathbf{c}_i\mathsf{U}\,\mathbf{c}_i = u_i\mathbf{c}_i \cdot \mathbf{c}_i = u_i$. Hence, Eq. (3.5) becomes

$$\begin{aligned} \mathbf{b} &= \mathbf{c}_1\cos(\zeta_0/2) + \mathbf{c}_2\sin(\zeta_0/2), \\ \mathbf{b}' &= \mathbf{c}_1\cos(\zeta_0/2) - \mathbf{c}_2\sin(\zeta_0/2), \end{aligned} \tag{3.16}$$

and, in view of Eqs. (3.6) and (3.14),

$$\mathbf{a} = \mathbf{e}_2, \quad \mathbf{a}' = \mathbf{e}_1, \tag{3.17}$$

where

$$\mathbf{e}_i = \frac{\mathsf{T}\mathbf{c}_i}{\sqrt{u_i}} = -\mathsf{R}\,\mathbf{c}_i \quad (i = 1, 2). \tag{3.18}$$

The vectors $\mathbf{e}_1$ and $\mathbf{e}_2$ are orthonormal, since R is a rotation matrix.

The optimal detector configuration given by Eqs. (3.16) and (3.17) is not unique. To obtain all possible detector configurations providing Eq. (3.11), we derive Eq. (3.10), as follows. Let $\mathbf{c}_3'$ be a unit vector orthogonal to $\mathbf{c}_1'$ and $\mathbf{c}_2'$; then $\mathbf{c}_i' = \sum_{j=1}^{3}\mathsf{W}_{ij}\mathbf{c}_j$ $(i = 1, 2, 3)$, where W is an orthogonal 3×3 matrix, $\mathsf{W}^T\mathsf{W} = I_3$. We have

$$\mathbf{c}_3'\mathsf{U}\,\mathbf{c}_3' = \mathsf{W}_{31}^2 u_1 + \mathsf{W}_{32}^2 u_2 + \mathsf{W}_{33}^2 u_3 \geq u_3, \tag{3.19}$$

since $\mathsf{W}_{31}^2 + \mathsf{W}_{32}^2 + \mathsf{W}_{33}^2 = 1$ and $u_3 \leq u_1 + u_2$. Moreover,

$$\sum_{i=1}^{3}\mathbf{c}_i'\mathsf{U}\,\mathbf{c}_i' = \mathrm{Tr}\,\mathsf{U} = u_1 + u_2 + u_3. \tag{3.20}$$

Equations (3.19) and (3.20) imply that $\mathbf{c}_1'\mathsf{U}\,\mathbf{c}_1' + \mathbf{c}_2'\mathsf{U}\,\mathbf{c}_2' = u_1 + u_2 + u_3 - \mathbf{c}_3'\mathsf{U}\,\mathbf{c}_3' \leq u_1 + u_2$. Hence, the maximum (3.10) is achieved when the expression (3.19) is minimal, i.e., equals u_3, which occurs for $\mathsf{W}_{31} = \mathsf{W}_{32} = 0$ and $\mathsf{W}_{33} = \pm 1$, i.e., for $\mathbf{c}_3' = \pm\mathbf{c}_3$. In this case $\mathbf{c}_1'$ and $\mathbf{c}_2'$ are an arbitrary pair of orthonormal vectors in the plane defined by $\mathbf{c}_1$ and $\mathbf{c}_2$. All such $\mathbf{c}_1'$ and $\mathbf{c}_2'$ are given by

$$\mathbf{c}_1' = \mathbf{c}_1\cos\eta \pm \mathbf{c}_2\sin\eta, \quad \mathbf{c}_2' = -\mathbf{c}_1\sin\eta \pm \mathbf{c}_2\cos\eta. \tag{3.21}$$

Here η is the arbitrary angle between $\mathbf{c}_1'$ and $\mathbf{c}_1$, and the two signs before $\mathbf{c}_2$ correspond to a reflection of $\mathbf{c}_1'$ and $\mathbf{c}_2'$ with respect to the $\mathbf{c}_1$ axis. The above derivation implies that no pair of unit orthogonal vectors $\mathbf{c}_1'$ and $\mathbf{c}_2'$ other than those in Eq. (3.21) can satisfy the condition (3.10), unless u_3 equals u_1 or u_2 (the latter cases are discussed in Sect. 3.4).

Inserting Eq. (3.21) into Eqs. (3.5) and (3.6) and taking into account Eq. (3.18), we obtain all detector configurations maximizing S, as follows,

$$
\begin{aligned}
\mathbf{a} &= (-\mathbf{e}_1\sqrt{u_1}\sin\eta \pm \mathbf{e}_2\sqrt{u_2}\cos\eta)/|\mathsf{T}\mathbf{c}_2'|,\\
\mathbf{a}' &= (\mathbf{e}_1\sqrt{u_1}\cos\eta \pm \mathbf{e}_2\sqrt{u_2}\sin\eta)/|\mathsf{T}\mathbf{c}_1'|,\\
\mathbf{b} &= \mathbf{c}_1\cos[\eta+\zeta_b(\eta)/2] \pm \mathbf{c}_2\sin[\eta+\zeta_b(\eta)/2],\\
\mathbf{b}' &= \mathbf{c}_1\cos[\eta-\zeta_b(\eta)/2] \pm \mathbf{c}_2\sin[\eta-\zeta_b(\eta)/2].
\end{aligned}
\tag{3.22}
$$

In Eq. (3.22) the upper (or lower) signs should be used simultaneously. The quantities $|\mathsf{T}\mathbf{c}_1'|$ and $|\mathsf{T}\mathbf{c}_2'|$ are given by

$$
|\mathsf{T}\mathbf{c}_{1(2)}'| = \sqrt{\frac{u_1+u_2 \pm (u_1-u_2)\cos 2\eta}{2}}, \tag{3.23}
$$

where the upper (lower) sign corresponds to $|\mathsf{T}\mathbf{c}_1'|$ ($|\mathsf{T}\mathbf{c}_2'|$). Inserting Eq. (3.23) into Eq. (3.7) and performing trigonometric calculations yields

$$
\zeta_b(\eta) = \arccos\left(\frac{u_1-u_2}{u_1+u_2}\cos 2\eta\right). \tag{3.24}
$$

Equation (3.24) can be compared with the angle ζ_a between $\mathbf{a}$ and $\mathbf{a}'$, satisfying $\cos\zeta_a = \mathbf{a}\cdot\mathbf{a}'$. As follows from Eqs. (3.22) and (3.23) and some calculations,

$$
\zeta_a(\eta) = \operatorname{arccot}\left(\frac{u_2-u_1}{2\sqrt{u_1u_2}}\sin 2\eta\right) \tag{3.25}
$$

(we assume that $0<\zeta_a,\zeta_b<\pi$). Equations (3.24) and (3.25) imply that the angles ζ_a and ζ_b vary with η between the values ζ_0 (3.15) and $\pi-\zeta_0$ with the period π. In particular, for $\eta = 0, \pm\pi/2, \pm\pi$ ($\eta = \pm\pi/4, \pm3\pi/4$) one gets $\zeta_a = \pi/2$ ($\zeta_b = \pi/2$), whereas ζ_b (ζ_a) acquires a maximal or minimal value. Moreover, Eqs. (3.22)–(3.24) imply the relations

$$
\mathbf{a}'(\eta\pm\pi/2) = \pm\mathbf{a}(\eta), \quad \mathbf{b}'(\eta\pm\pi/2) = \pm\mathbf{b}(\eta), \tag{3.26}
$$

whereas $\mathbf{a}$, $\mathbf{a}'$, $\mathbf{b}$, and $\mathbf{b}'$ change the sign for $\eta\to\eta+\pi$.

As follows from Eq. (3.22), the set of all optimal configurations maximizing S for a given state generally depends on one continuous parameter (η) and one discrete parameter [which corresponds to the two possible signs in Eq. (3.22)]. However, when u_3 is equal to u_1 and/or u_2 (a degenerate case), the set of optimal configurations is characterized by two or three continuous parameters, as discussed in Sect. 3.4.

Note that the optimal detector orientations (3.22) depend on u_1 and u_2 only through the ratio u_2/u_1. As a result, two different states with the same R, $\mathbf{c}_1$, $\mathbf{c}_2$, and u_2/u_1 have the same or, at least, overlapping sets of optimal detector configurations. (The overlap may be incomplete only when, at least, for one of the states $u_1 = u_3$ or $u_2 = u_3$.) In particular, for the states ρ and ρ' with the matrices T and T', respectively, satisfying $\mathsf{T}' = f\mathsf{T}$ $(f > 0)$, the respective quantities S_+ and S'_+ obey $S'_+ = fS_+$, whereas the optimal configurations are the same for both states. An example of such states ρ and ρ' is given by the input and output states of the depolarizing channel [42],

$$\rho' = f\rho + (1-f)\frac{I_4}{4} \quad (0 < f \leq 1). \tag{3.27}$$

3.3 Polar coordinates

According to Eq. (3.22), the optimal detector directions for qubits a and b are confined to the planes $(\mathbf{e}_1, \mathbf{e}_2)$ and $(\mathbf{c}_1, \mathbf{c}_2)$, respectively. It is convenient to specify these directions by means of polar angles.

To this end, we introduce the polar coordinate ν in the $(\mathbf{c}_1, \mathbf{c}_2)$ plane, which is counted from $\mathbf{c}_1$ in the direction where $\nu = \pi/2$ corresponds to $\mathbf{c}_2$, and the polar coordinate δ in the $(\mathbf{e}_1, \mathbf{e}_2)$ plane [differing generally from the $(\mathbf{c}_1, \mathbf{c}_2)$ plane], which is counted from $\mathbf{e}_1$ in the direction where $\delta = \pi/2$ is the polar coordinate of $\mathbf{e}_2$. Then Eq. (3.22) can be recast in the form

$$\begin{aligned}
\mathbf{a} &= \mathbf{e}_1 \cos[\delta_a(\eta)] \pm \mathbf{e}_2 \sin[\delta_a(\eta)],\\
\mathbf{a}' &= \mathbf{e}_1 \cos[\delta'_a(\eta)] \pm \mathbf{e}_2 \sin[\delta'_a(\eta)],\\
\mathbf{b} &= \mathbf{c}_1 \cos[\nu_b(\eta)] \pm \mathbf{c}_2 \sin[\nu_b(\eta)],\\
\mathbf{b}' &= \mathbf{c}_1 \cos[\nu'_b(\eta)] \pm \mathbf{c}_2 \sin[\nu'_b(\eta)].
\end{aligned} \tag{3.28}$$

Here $\delta_a,\ \delta'_a,\ \nu_b$, and ν'_b $(-\delta_a,\ -\delta'_a,\ -\nu_b$, and $-\nu'_b)$ are the polar coordinates of the vectors $\mathbf{a},\ \mathbf{a}',\ \mathbf{b}$, and $\mathbf{b}'$, respectively, when the upper (lower) sign in Eq. (3.28) is realized. Thus, Eq. (3.28) implies that an optimal qubit configuration changes to another optimal configuration under the sign change of the polar angles

$$(\delta_a, \delta'_a, \nu_b, \nu'_b) \to (-\delta_a, -\delta'_a, -\nu_b, -\nu'_b). \tag{3.29}$$

The configurations corresponding to the two different choices of the sign in Eq. (3.22) or (3.28) transform to each other by the reflection of the detector axes for qubits a and b with respect to the axes $\mathbf{e}_1$ and $\mathbf{c}_1$, respectively.

The functions $\delta_a(\eta),\ \delta'_a(\eta),\ \nu_b(\eta)$, and $\nu'_b(\eta)$ satisfy the relations [see Eq. (3.26)]

$$\delta_a(\eta) = \delta'_a(\eta + \pi/2), \tag{3.30}$$

$$\nu_b(\eta) = \nu'_b(\eta + \pi/2). \tag{3.31}$$

These functions can be obtained as follows. On comparing Eqs. (3.22) and (3.28) with the upper signs, it is easy to see that

$$\nu_b(\eta) = \eta + \zeta_b(\eta)/2, \quad \nu'_b(\eta) = \eta - \zeta_b(\eta)/2. \tag{3.32}$$

This implies that $\eta = (\nu_b + \nu_b')/2$, yielding a geometric interpretation of the parameter η: η equals the polar coordinate of the bisector of the angle between $\mathbf{b}$ and $\mathbf{b}'$ when the upper sign in Eq. (3.22) or (3.28) is realized.

Let us now obtain $\delta_a(\eta)$ and $\delta_a'(\eta)$. The second Eq. (3.22) implies that

$$\begin{aligned} \cos\delta_a' &= \mathbf{a}'\cdot\mathbf{e}_1 = \sqrt{u_1}\cos\eta/|\mathsf{T}\mathbf{c}_1'|, \\ \sin\delta_a' &= \mathbf{a}'\cdot\mathbf{e}_2 = \sqrt{u_2}\sin\eta/|\mathsf{T}\mathbf{c}_1'|. \end{aligned} \tag{3.33}$$

yielding

$$\delta_a'(\eta) = \arctan\left(\sqrt{\frac{u_2}{u_1}}\tan\eta\right) \quad (-\pi/2 \le \eta \le \pi/2). \tag{3.34}$$

The right-hand sides of Eqs. (3.33) are continuous functions of η, which implies that δ_a' is also a continuous function of η. A continuous extension of $\delta_a'(\eta)$ beyond the interval $-\pi/2 \le \eta \le \pi/2$ and Eq. (3.30) provide the detector angles for qubit a,

$$\delta_a(\eta) = \delta_a'(\eta + \pi/2), \quad \delta_a'(\eta) = \arctan\left(\sqrt{\frac{u_2}{u_1}}\tan\eta\right) + \operatorname{nint}\left(\frac{\eta}{\pi}\right)\pi, \tag{3.35}$$

where $\operatorname{nint}(\eta/\pi)$ is the nearest integer to η/π.

Figure 1 shows the dependence on η of the polar coordinates of the observation axes in Eq. (3.28) with the upper signs for $u_2/u_1 = 0.3$ ($\zeta_0 \approx 1.00$). Our calculations show that the set of the polar coordinates of the detectors is always ordered as follows (cf. Fig. 1),

$$\delta_a > \nu_b > \delta_a' > \nu_b'. \tag{3.36}$$

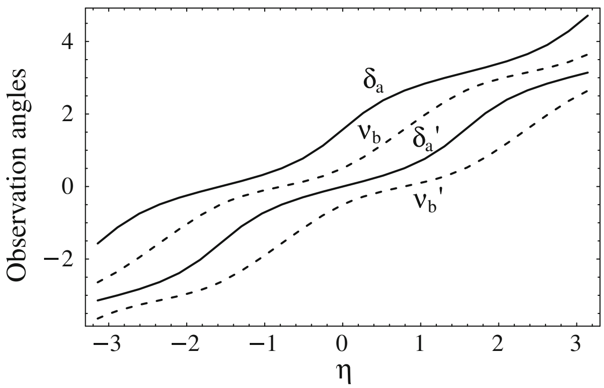

Fig. 1 Polar angles of the detector axes versus η for $u_2/u_1 = 0.3$ ($\zeta_0 \approx 1.00$), as given by Eqs. (3.32) and (3.35)

3.3.1 Symmetry with respect to the exchange of the qubits

In the above derivation in Sect. 3.1 the observables for qubit b are treated differently from those for qubits a, resulting in different solutions for the two qubits [cf., e.g., Eqs. (3.24) and (3.25)]. To check whether these solutions are invariant with respect to the qubit swap, we rewrite Eq. (3.3) in the form

$$S = \mathbf{b}\mathsf{T}^T\mathbf{a} - \mathbf{b}\mathsf{T}^T\mathbf{a}' + \mathbf{b}'\mathsf{T}^T\mathbf{a} + \mathbf{b}'\mathsf{T}^T\mathbf{a}', \tag{3.37}$$

where the roles of qubits a and b are interchanged. As follows from Eq. (3.14), $\mathsf{T}^T = -\sqrt{\mathsf{U}}\,\mathsf{R}^T = -\mathsf{R}^T\mathsf{R}\sqrt{\mathsf{U}}\,\mathsf{R}^T = \mathsf{R}^T\mathsf{T}\mathsf{R}^T$, and hence $\mathbf{b}\mathsf{T}^T\mathbf{a} = \mathbf{b}(\mathsf{R}^T\mathsf{T}\mathsf{R}^T)\mathbf{a} = (\mathsf{R}\,\mathbf{b})\mathsf{T}(\mathsf{R}^T\mathbf{a})$. Thus, Eq. (3.37) can be recast as

$$S = (\mathsf{R}\,\mathbf{b})\mathsf{T}(\mathsf{R}^T\mathbf{a}) - (\mathsf{R}\,\mathbf{b}')\mathsf{T}(\mathsf{R}^T\mathbf{a}) + (\mathsf{R}\,\mathbf{b})\mathsf{T}(\mathsf{R}^T\mathbf{a}') + (\mathsf{R}\,\mathbf{b}')\mathsf{T}(\mathsf{R}^T\mathbf{a}'). \tag{3.38}$$

Comparing Eqs. (3.3) and (3.38), we obtain that S is invariant under the substitution

$$(\mathbf{a}, \mathbf{a}', \mathbf{b}, \mathbf{b}') \to (\mathsf{R}\,\mathbf{b}', \mathsf{R}\,\mathbf{b}, \mathsf{R}^T\mathbf{a}', \mathsf{R}^T\mathbf{a}) \tag{3.39}$$

or

$$(\mathbf{a}, \mathbf{a}', \mathbf{b}, \mathbf{b}') \to (-\mathsf{R}\,\mathbf{b}', -\mathsf{R}\,\mathbf{b}, -\mathsf{R}^T\mathbf{a}', -\mathsf{R}^T\mathbf{a}). \tag{3.40}$$

In view of Eq. (2.11), one of the symmetry relations (3.39) and (3.40) is a consequence of the other.

With the help of Eqs. (3.18) and (3.28), we obtain that Eq. (3.40) is equivalent to the inversion of the order of the detector coordinates,

$$(\delta_a, \delta_a', \nu_b, \nu_b') \to (\nu_b', \nu_b, \delta_a', \delta_a), \tag{3.41}$$

where the quantities in the parentheses are the respective polar angles of the vectors $(\mathbf{a}, \mathbf{a}', \mathbf{b}, \mathbf{b}')$. Our numerical calculations show that if $(\delta_a, \delta_a', \nu_b, \nu_b')$ is an optimal detector configuration corresponding to the upper (lower) signs in Eq. (3.28), then $(\nu_b', \nu_b, \delta_a', \delta_a)$ is an optimal configuration corresponding to the lower (upper) signs in Eq. (3.28).

In summary, the set of the optimal detector configurations is invariant with respect to the qubit-swap symmetry relation (3.41). Thus, there are, at least, three simple relations between different optimal configurations, Eqs. (2.11), (3.29), and (3.41).

3.4 Degenerate cases

Consider the optimal detector configurations for states characterized by the matrix U with degenerate eigenvalues.

3.4.1 Completely degenerate case ($u_1 = u_2 = u_3 \equiv u$)

Now $\mathsf{U} = uI_3$, and Eq. (3.11) yields $S_+ = 2\sqrt{2u}$, so that the BI is violated for

$$u > 1/2. \tag{3.42}$$

Now Eq. (3.14) becomes

$$\mathsf{T} = -\sqrt{u}\mathsf{R}. \tag{3.43}$$

In this case any two perpendicular unit vectors can be chosen as $\mathbf{c}_1$ and $\mathbf{c}_2$. Then Eqs. (3.18), (3.22)–(3.24) yield that all detector configurations providing S_+ are given by the expressions

$$\mathbf{a} = \frac{\mathsf{R}\,\mathbf{b}' - \mathsf{R}\,\mathbf{b}}{\sqrt{2}}, \quad \mathbf{a}' = -\frac{\mathsf{R}\,\mathbf{b} + \mathsf{R}\,\mathbf{b}'}{\sqrt{2}}, \tag{3.44}$$

where $\mathbf{b}$ and $\mathbf{b}'$ are arbitrary mutually perpendicular unit vectors. Since the orientation of the pair of orthogonal vectors $\mathbf{b}$ and $\mathbf{b}'$ is characterized by three angles, in the completely degenerate case the set of optimal configurations is characterized by three continuous parameters.

The class of states possessing U with completely degenerate eigenvalues includes all pure maximally entangled states. For such states $u = 1$ and hence $S_+ = 2\sqrt{2}$ [cf. Eq. (2.12)]. Since for such states $\mathbf{r}_a = \mathbf{r}_b = 0$, a maximally entangled state is uniquely determined by $\mathsf{T} = -\mathsf{R}$ [cf. Eq. (3.43)]. The simplest example of such a state is the singlet state $|\Psi_-\rangle$ [Eq. (2.14)], which is often considered in connection with the BI. For the singlet state Eq. (3.2) yields $\mathsf{T} = -I_3$, i.e., $\mathsf{R} = I_3$, and Eq. (3.44) becomes [32]

$$\mathbf{a} = \frac{\mathbf{b}' - \mathbf{b}}{\sqrt{2}}, \quad \mathbf{a}' = -\frac{\mathbf{b} + \mathbf{b}'}{\sqrt{2}}. \tag{3.45}$$

An example of a mixed state corresponding to the completely degenerate case is the Werner state [60]

$$\rho = \sqrt{u}|\Psi_-\rangle\langle\Psi_-| + (1 - \sqrt{u})\frac{I_4}{4}, \tag{3.46}$$

which is a special case of the state (3.27). The BI violation condition (3.42) for this state was obtained in [27]. For the state (3.46) $\mathsf{T} = -\sqrt{u}I_3$, yielding $\mathsf{R} = I_3$, and we obtain the same optimal configurations (3.45) as for the singlet.

3.4.2 Case $u_1 = u_3$ or $u_2 = u_3$

In this case we assume for definiteness that $u_2 = u_3 < u_1$. Then $\mathbf{c}_1$ is defined uniquely, whereas $\mathbf{c}_2$ can be any unit radius-vector in the plane perpendicular to $\mathbf{c}_1$. Now the set of optimal configurations (3.22) or (3.28) is characterized by two continuous parameters, η and an angle specifying the direction of $\mathbf{c}_2$ in the plane $(\mathbf{c}_2, \mathbf{c}_3)$ with respect to some reference axis. In this case the discrete parameter is replaced by the new continuous parameter; indeed, now one of the two possible signs in Eqs. (3.22) and (3.28) can be omitted, since it is recovered for $\mathbf{c}_2 \to -\mathbf{c}_2$.

3.4.3 Case $u_3 < u_1 = u_2 \equiv u$

In this case Eq. (3.11) yields $S_+ = 2\sqrt{2u}$, as in the completely degenerate case. Now any two perpendicular unit vectors can be chosen as $\mathbf{c}_1$ and $\mathbf{c}_2$ in the plane of the eigenvectors of U corresponding to the degenerate eigenvalue $u_1 = u_2$. Then Eqs. (3.18), (3.22)–(3.24) yield that all detector configurations providing S_+ are given by Eq. (3.44), where $\mathbf{b}$ and $\mathbf{b}'$ are arbitrary mutually perpendicular unit vectors in the plane determined by $\mathbf{c}_1$ and $\mathbf{c}_2$. In other words, now the optimal configurations are a subset of the set of the optimal configurations for the maximally entangled state characterized by the rotation matrix R. The optimal configurations are described by the following polar angles [see Eqs. (3.32) and (3.35)],

$$\delta_a = \eta + \pi/2,\ \ \delta_a' = \eta,\ \ \nu_b = \eta + \pi/4,\ \ \nu_b' = \eta - \pi/4, \tag{3.47}$$

and by Eq. (3.29). Now the set of optimal configurations is characterized by one continuous parameter and one discrete parameter as in the nondegenerate case.

3.5 Special cases

Here we provide all optimal detector configurations for the states with T assuming one of the two simple forms,

$$\mathsf{T} = \mathrm{diag}(\tau_x, \tau_x, -\tau_z), \tag{3.48}$$
$$\mathsf{T} = \mathrm{diag}(\tau_x, -\tau_x, \tau_z). \tag{3.49}$$

The cases (3.48) and (3.49) are of interest since they describe the important classes of odd and even states (see below Sect. 4.4.2). In view of Eq. (B.6), the most general two-qubit states with T given by Eq. (3.48) or (3.49) are described by Eq. (B.5) with $\rho_{14} = 0$ or $\rho_{23} = 0$, respectively, so that in Eq. (3.48) [(3.49)] $\tau_x = 2\rho_{23}$ and $\tau_z = 2\rho_{22} + 2\rho_{33} - 1$ ($\tau_x = 2\rho_{14}$ and $\tau_z = 1 - 2\rho_{22} - 2\rho_{33}$). We assume below the validity of a necessary condition for the BI violation, $\det(\mathsf{T}) < 0$ (Sect. 3.1), which implies $\tau_x \neq 0$ and $\tau_z > 0$. The latter inequality is equivalent to the conditions $\rho_{22} + \rho_{33} > 1/2$ and $\rho_{22} + \rho_{33} < 1/2$ for the cases (3.48) and (3.49), respectively. Without a loss of generality, we focus on the states with $\tau_x > 0$ in Eqs. (3.48) and (3.49).[4] Thus we require that in Eqs. (3.48)and (3.49)

[4] One can make ρ_{23} and ρ_{14} nonnegative in Eq. (B.5) by a local transformation. For instance, the π rotation of one of the qubits around the z axis changes the signs of ρ_{23} and ρ_{14}, whereas the $\pi/2z$-rotations of the qubits change the sign of ρ_{14}.

$$\tau_x > 0, \quad \tau_z > 0. \tag{3.50}$$

In both cases (3.48) and (3.49) $\mathsf{U} = \mathrm{diag}(\tau_x^2, \tau_x^2, \tau_z^2)$, yielding, in view of Eq. (3.11),

$$S_+ = 2\max\left\{\sqrt{2}\tau_x, \sqrt{\tau_x^2 + \tau_z^2}\right\}, \tag{3.51}$$

i.e., $S_+ = 2\sqrt{2}\tau_x$ for $\tau_x \geq \tau_z$ and $S_+ = 2\sqrt{\tau_x^2 + \tau_z^2}$ for $\tau_x \leq \tau_z$. However, the optimal detector configurations are different in the cases (3.48) and (3.49), as follows.

3.5.1 Case (3.48)

In the case (3.48) $\mathsf{R} = \mathrm{diag}(-1, -1, 1)$. There are three possibilities, as follows.

a. If $\tau_x \geq \tau_z$, $u_1 = u_2 = \tau_x^2$, and one can choose as $\mathbf{c}_1$ and $\mathbf{c}_2$ any two unit perpendicular radius-vectors in the xy plane (see Sect. 3.4.3). We choose $\mathbf{c}_1 = \mathbf{x}$ and $\mathbf{c}_2 = \mathbf{y}$, where $\mathbf{x}$, $\mathbf{y}$, and $\mathbf{z}$ denote the unit vectors along the corresponding axes. Now $\mathbf{e}_1$ ($\mathbf{e}_2$) coincides with $\mathbf{c}_1$ ($\mathbf{c}_2$), yielding $\delta = \nu = \phi$, where ϕ is the polar coordinate in the horizontal (xy) plane. The optimal configurations lie in the horizontal plane, being given by

$$(\phi_a, \phi_a', \phi_b, \phi_b') = \pm(0, \pi/2, \pi/4, 3\pi/4) + C, \tag{3.52}$$

where C is an arbitrary real number. Equation (3.52) follows from Eq. (3.47), where we introduced the double sign to take into account both signs in Eq. (3.28) [cf. Eq. (3.29)]. Hence, Eq. (3.52) describes all optimal configurations for $\tau_x > \tau_z$.

b. If $\tau_x \leq \tau_z$, we choose

$$u_1 = \tau_z^2, \quad u_2 = u_3 = \tau_x^2. \tag{3.53}$$

Then $\mathbf{c}_1 = -\mathbf{e}_1 = \mathbf{z}$. Since $u_2 = u_3$ (see Sect. 3.4.2), we choose $\mathbf{c}_2 = \mathbf{e}_2 = \mathbf{x}\cos\phi_0 + \mathbf{y}\sin\phi_0$, where ϕ_0 is an arbitrary number which equals the polar angle of $\mathbf{c}_2$ in the xy plane. The above expressions for $\mathbf{c}_1$, $\mathbf{c}_2$, $\mathbf{e}_1$, and $\mathbf{e}_2$ imply that the polar coordinates δ and ν satisfy the relation

$$\nu = \pi - \delta = \theta. \tag{3.54}$$

Here θ is the polar angle in a vertical plane (a plane passing through the z axis), which makes the angle ϕ_0 with the x axis; θ is counted from the z axis in the direction where $\theta = \pi/2$ corresponds to $\mathbf{c}_2$. The polar coordinates of the optimal detector axes θ_a, θ_a', θ_b, and θ_b' as functions of the parameter η can be obtained from Eqs. (3.29), (3.32), (3.35), (3.53), and (3.54), namely,

$$\theta_a(\eta) = \theta_a'(\eta + \pi/2), \quad \theta_a'(\eta) = \pi \mp \left[\arctan\left(\frac{\tau_x}{\tau_z}\tan\eta\right) + \mathrm{nint}\left(\frac{\eta}{\pi}\right)\pi\right], \tag{3.55}$$

$$\theta_b(\eta) = \pm[\eta + \zeta_b(\eta)/2], \qquad \theta_b'(\eta) = \pm[\eta - \zeta_b(\eta)/2], \tag{3.56}$$

where, in view of Eq. (3.24),

$$\zeta_b(\eta) = \arccos\left(\frac{\tau_z^2 - \tau_x^2}{\tau_z^2 + \tau_x^2}\cos 2\eta\right). \tag{3.57}$$

In Eqs. (3.55) and (3.56) the upper (or lower) signs should be used simultaneously; they correspond to the upper (lower) signs in Eq. (3.28).

Thus, now optimal configurations lie in any vertical plane; they are characterized by two continuous parameters, η and ϕ_0, in agreement with Sect. 3.4.2. As discussed above, the optimal configurations are horizontal for $\tau_x > \tau_z$ and vertical for $\tau_x < \tau_z$.

c. For $\tau_x = \tau_z$ we have the completely degenerate case (Sect. 3.4.1) with $\mathsf{R} = \mathrm{diag}(-1, -1, 1)$ describing the rotation by π around the z axis. This rotation of qubit a yields $|\Psi_-\rangle \to |\Psi_+\rangle$. Hence, in this case the optimal configurations coincide with those for the Bell state $|\Psi_+\rangle$ (2.14) (see Sect. 3.4.1). These configurations [32] include, in particular, the horizontal configurations given by Eq. (3.52) and the vertical configurations which follow from Eqs. (3.47) and (3.54) and can be cast as

$$(\theta_a, \theta_a') = \pm(0, \pi/2) - C, \quad (\theta_b, \theta_b') = \pm(3\pi/4, \pi/4) + C. \tag{3.58}$$

Here we introduced the double sign as in Eq. (3.52).

3.5.2 Case (3.49)

In the case (3.49) $\mathsf{R} = \mathrm{diag}(-1, 1, -1)$. There are three possibilities, as follows.

a. If $\tau_x \geq \tau_z$, $u_1 = u_2 = \tau_x^2$, and we can choose $\mathbf{c}_1 = \mathbf{e}_1 = \mathbf{x}$ and $\mathbf{c}_2 = -\mathbf{e}_2 = \mathbf{y}$, yielding $\nu = -\delta = \phi$. In this case the optimal configurations lie in the horizontal plane and are given by Eq. (3.52) with $\phi_a \to -\phi_a$ and $\phi_a' \to -\phi_a'$, i.e., by

$$(\phi_a, \phi_a') = \pm(0, -\pi/2) - C, \quad (\phi_b, \phi_b') = \pm(\pi/4, 3\pi/4) + C. \tag{3.59}$$

b. For $\tau_x \leq \tau_z$ Eq. (3.53) holds. As above, $\mathbf{c}_1 = \mathbf{e}_1 = \mathbf{z}$ and $\mathbf{c}_2 = \mathbf{x}\cos\phi_0 + \mathbf{y}\sin\phi_0$, but $\mathbf{e}_2 = \mathbf{x}\cos\phi_0 - \mathbf{y}\sin\phi_0$. Now the optimal detector axes for qubits a and b lie generally in different vertical planes characterized, respectively, by the polar coordinates ϕ_a and ϕ_b (in the xy plane) of $\mathbf{c}_2$ and $\mathbf{e}_2$, respectively, such that

$$\phi_b = -\phi_a = \phi_0. \tag{3.60}$$

For a given value of ϕ_0, the optimal configurations are given by Eqs. (3.32), (3.35), (3.29), (3.53), and (3.57).

In particular, the detectors are coplanar in two cases. For $\phi_0 = 0$ and π the optimal configurations lie in the xz plane, the polar coordinates satisfying

$$\nu = \delta = \theta, \tag{3.61}$$

whereas for $\phi_0 = \pi/2$ and $3\pi/2$ they lie in the yz plane and

$$\nu = -\delta = \theta. \tag{3.62}$$

In Eqs. (3.61) and (3.62) θ is counted from $\mathbf{z}$ in the direction where $\theta = \pi/2$ corresponds to $\mathbf{x}$ and $\mathbf{y}$, respectively. In the cases (3.61) and (3.62), the optimal configurations for qubit a are given, respectively, by the equations [cf. Eqs. (3.55)]

$$\theta_a(\eta) = \theta_a'(\eta + \pi/2), \quad \theta_a'(\eta) = \pm\left[\arctan\left(\frac{\tau_x}{\tau_z}\tan\eta\right) + \mathrm{nint}\left(\frac{\eta}{\pi}\right)\pi\right] \tag{3.63}$$

and

$$\theta_a(\eta) = \theta_a'(\eta + \pi/2), \quad \theta_a'(\eta) = \mp\left[\arctan\left(\frac{\tau_x}{\tau_z}\tan\eta\right) + \mathrm{nint}\left(\frac{\eta}{\pi}\right)\pi\right], \tag{3.64}$$

whereas the optimal configurations for qubit b are given by Eqs. (3.56) for both cases (3.61) and (3.62).

c. In the completely degenerate case $\tau_x = \tau_z$ the optimal configurations coincide with those for the maximally entangled state characterized by $\mathsf{R} = \mathrm{diag}(-1, 1, -1)$ (see Sect. 3.4.1). This state, obtained from the singlet by the π rotation of qubit a around the y axis, is $|\Phi_+\rangle$ [Eq. (2.13)]. In particular, the horizontal optimal configurations for $|\Phi_+\rangle$ are given by Eq. (3.59), whereas the vertical optimal configurations are given by Eqs. (3.47) and (3.29),

$$(\delta_a, \delta_a', \nu_b, \nu_b') = \pm(0, \pi/2, \pi/4, 3\pi/4) + C. \tag{3.65}$$

In the planar cases Eq. (3.65) simplifies according to Eqs. (3.61) and (3.62).

Note that Eq. (3.49) follows from Eq. (3.48) under the π rotation of qubit a around the x axis. As a result, the above optimal configurations for the case (3.49) can be obtained from those discussed in Sect. 3.5.1 by the π rotation of the detector axes for qubit a around the x axis.

4 Effects of decoherence

4.1 Description of decoherence

To investigate effects of decoherence on the BI violation, we assume the following simplified picture of the experiment: after a fast preparation of the initial state ρ_0, the qubits undergo decoherence during time t resulting in the state ρ, then a fast measurement follows. Now in Eq. (2.4)

$$\rho = \mathscr{L}(\rho_0), \tag{4.1}$$

where the superoperator (linear map) $\mathscr{L}$ describes decoherence of the qubit pair. We assume independent (local) decoherence of each qubit and the absence of any other evolution, so that

$$\mathscr{L} = \mathscr{L}_a \otimes \mathscr{L}_b. \tag{4.2}$$

We consider Markovian decoherence which involves energy relaxation at the zero temperature (i.e., spontaneous transitions $|1\rangle \to |0\rangle$) and pure dephasing. The assumption of the zero temperature, $T = 0$, is applicable to low-temperature systems (such as superconducting phase qubits), with $k_B T \ll E_q$, where k_B is the Boltzmann constant and E_q is the energy separation of the qubit. Note, however, that the BI violation conditions were found in [33] to depend very weakly on the temperature. Under the above assumptions, the elements of the density matrix $\rho_k(t)$ of qubit k ($k = a, b$) obey the Bloch equations [19]

$$\begin{aligned} &\dot{\rho}_{11}^k(t) = -\dot{\rho}_{00}^k(t) = -\rho_{11}^k(t)/T_1^k, \\ &\dot{\rho}_{10}^k(t) = -\rho_{10}^k(t)/T_2^k, \quad \dot{\rho}_{01}^k(t) = -\rho_{01}^k(t)/T_2^k. \end{aligned} \tag{4.3}$$

Here T_1^k and T_2^k are the decoherence times, obeying $T_2^k \le 2T_1^k$, where the inequality occurs in the presence of pure dephasing which proceeds with the rate $\Gamma_d^k = 1/T_2^k - 1/(2T_1^k)$. In the derivation of Eqs. (4.3) it is usually assumed that $E_q/\hbar \gg 1/T_1^k, 1/T_2^k$. This condition is satisfied in many systems. In particular, it holds for superconducting phase qubits.

Equations (4.3) are usually used to describe environmentally induced (or extrinsic) decoherence, which can be contrasted with the so called intrinsic decoherence, introduced via a modification of the Schrödinger equation in order to solve some fundamental difficulties in our understanding of quantum mechanics [40]. Note, however, that the model in [40] in the first order in the expansion parameter, as well as other models of intrinsic decoherence (see references in [40]), are formally equivalent to proper dephasing. Hence, the present paper describes effects of both extrinsic and intrinsic decoherence.

Equations (4.3) can be easily solved, providing the linear map $\rho_k(t) = \mathscr{L}_k(\rho_k(0))$. The superoperator $\mathscr{L}_k$ can be written in terms of the Kraus operators (the operator-product form [42]),

$$\mathscr{L}_k(\rho_k(0)) = \sum_{i=1}^{3} K_i^k \rho_k(0) (K_i^k)^\dagger, \tag{4.4}$$

where the Kraus operators are the special case for $T = 0$ of the Kraus operators obtained in [33], namely[1]

$$\begin{aligned} &K_1^k = \begin{pmatrix} 0 & \sqrt{1-\gamma_k} \\ 0 & 0 \end{pmatrix}, \quad K_2^k = \begin{pmatrix} \mu_k & 0 \\ 0 & \sqrt{\gamma_k} \end{pmatrix}, \\ &K_3^k = \begin{pmatrix} \sqrt{1-\mu_k^2} & 0 \\ 0 & 0 \end{pmatrix}. \end{aligned} \tag{4.5}$$

Here

$$\gamma_k = e^{-t/T_1^k}, \ \mu_k = \lambda_k/\sqrt{\gamma_k} = e^{-\Gamma_d^k t}, \ \lambda_k = e^{-t/T_2^k}. \tag{4.6}$$

The Kraus operators (4.5) take into account energy relaxation and pure dephasing simultaneously, extending thus the previously known Kraus operators [42] which describe either effect separately.

Combining Eqs. (4.1), (4.2), and (4.4) yields the expression for the two-qubit superoperator

$$\rho = \mathscr{L}(\rho_0) = \sum_{i,j=1}^{3} K_{ij}\rho_0 K_{ij}^{\dagger}, \quad K_{ij} = K_i^a \otimes K_j^b \tag{4.7}$$

through the nine two-qubit Kraus operators K_{ij}. As a result of decoherence, the initial two-qubit density matrix $\rho_0 = \{\rho_{ij}^0\}$ evolves after time t to

$$\rho = \begin{pmatrix} \rho_{11}^0 + \gamma_b'\rho_{22}^0 + \gamma_a'\rho_{33}^0 + \gamma_a'\gamma_b'\rho_{44}^0 & \lambda_b(\rho_{12}^0 + \gamma_a'\rho_{34}^0) & \lambda_a(\rho_{13}^0 + \gamma_b'\rho_{24}^0) & \lambda_a\lambda_b\rho_{14}^0 \\ \lambda_b(\rho_{21}^0 + \gamma_a'\rho_{43}^0) & \gamma_b(\rho_{22}^0 + \gamma_a'\rho_{44}^0) & \lambda_a\lambda_b\rho_{23}^0 & \lambda_a\gamma_b\rho_{24}^0 \\ \lambda_a(\rho_{31}^0 + \gamma_b'\rho_{42}^0) & \lambda_a\lambda_b\rho_{32}^0 & \gamma_a(\rho_{33}^0 + \gamma_b'\rho_{44}^0) & \gamma_a\lambda_b\rho_{34}^0 \\ \lambda_a\lambda_b\rho_{41}^0 & \lambda_a\gamma_b\rho_{42}^0 & \gamma_a\lambda_b\rho_{43}^0 & \gamma_a\gamma_b\rho_{44}^0 \end{pmatrix}, \tag{4.8}$$

where $\gamma_{a(b)}' = 1 - \gamma_{a(b)}$ and the values $i, j = 1, 2, 3, 4$ of the subscripts of ρ_{ij} correspond to the basis

$$\{|00\rangle, |01\rangle, |10\rangle, |11\rangle\}. \tag{4.9}$$

Decoherence generally breaks the invariance of S with respect to local transformations of the initial state ρ_0 and the corresponding rotations of the detectors [cf. Eq. (2.7)]. As a result, locally equivalent initial states may yield different maximal violations of the BI. However, in the present model of decoherence S is still invariant under transformations of ρ_0 due to local rotations of the qubits around the z axis and the corresponding rotations of the detectors.

4.2 Bell operator modified by decoherence

It is useful to recast Eq. (2.4), $S = \mathrm{Tr}\,(\mathscr{B}\rho)$, in the form

$$S = \mathrm{Tr}\,(\mathscr{B}_d\rho_0) \tag{4.10}$$

with the modified Bell operator $\mathscr{B}_d = (\mathscr{L}_a^* \otimes \mathscr{L}_b^*)(\mathscr{B})$ or

$$\mathscr{B}_d = A_d B_d - A_d B_d' + A_d' B_d + A_d' B_d'. \tag{4.11}$$

Here $\mathscr{L}_k^*$ $(k = a, b)$ is the map adjoint (dual) to $\mathscr{L}_k$ that moves observables of the quantum system [1] and

$$A_d = \mathscr{L}_a^*(A) = \sum_{i=1}^{3} (K_i^a)^\dagger A K_i^a, \tag{4.12}$$

etc. By combining Eqs. (2.6), (4.5), and (4.12) we obtain that

$$A_d = (1 - \gamma_a) a_z + \mathbf{q}_a \cdot \boldsymbol{\sigma}_a, \quad \mathbf{q}_a = (\lambda_a a_x, \lambda_a a_y, \gamma_a a_z), \tag{4.13}$$

where λ_k is defined in Eq. (4.6). Expressions similar to Eq. (4.13) hold also for A'_d, B_d, and B'_d. The maximal violation of the BI occurs always for a pure initial state (equal to an eigenvector of the Hermitian operator $\mathscr{B}_d$ corresponding to the maximal eigenvalue).

We performed numerical calculations of the maximum $S_{\max}$ of S over all the states and observation directions as a function of the decoherence parameters with the help of the Mathematica routine NMaximize. We used two methods.

The first method is based on the fact that $S_{\max}$ is equal to the maximum of the greatest eigenvalue of $\mathscr{B}_d$ over the directions $\mathbf{a}$, $\mathbf{a}'$, $\mathbf{b}$, and $\mathbf{b}'$, the optimal state being given by the corresponding eigenvector. The detector axes are determined by eight independent parameters, but the number of the varied parameters can be reduced to five, using the following facts. (i) The set of points corresponding to any unit vector in all optimal configurations is a great circle on the Bloch sphere (see Eq. (3.28); Fig. 1). Since all great circles intersect each other, one of the detectors can be fixed in any great circle; in our calculations, we place $\mathbf{a}$ in the xy plane. (ii) The invariance of S with respect to rotations of the qubits around the z axis (Sect. 4.1) allows us to set $\mathbf{a} = (1, 0, 0)$ and, say, $b_y = 0$.

The second method, based on the analytical approach of Sect. 3, is discussed in Sect. 4.3.

4.3 States maximizing the BI violation

It was shown in Sect. 2.3 that real states (2.23),

$$|\Psi\rangle = c_1|00\rangle + c_2|01\rangle + c_3|10\rangle + c_4|11\rangle, \tag{4.14}$$

provide maximal BI violations for given probabilities c_i^2. More generally, our numerical calculations by the method of Sect. 4.2 show that even in the presence of decoherence, $S_{\max}$ can be always obtained for an initial state of the form (4.14). The real states (4.14) form a subset, depending on 3 independent parameters, of the set of pure two-qubit states, depending on 6 independent parameters.

The most general state equivalent to Eq. (4.14) up to local qubit z-rotations has the form (with the accuracy to an overall phase factor)

$$|\Psi(\alpha_a, \alpha_b)\rangle = c_1|00\rangle + c_2 e^{i\alpha_b}|01\rangle + c_3 e^{i\alpha_a}|10\rangle + c_4 e^{i(\alpha_a+\alpha_b)}|11\rangle. \tag{4.15}$$

All optimal detector configurations for this state are obtained from those for the state (4.14) by rotating the detectors for qubits a and b around the z axis by the angles α_a and α_b, respectively [cf. Eqs. (2.7)]. As mentioned in Sect. 2.3, the class of states (4.15) includes all maximally entangled states.

It is convenient for numerical calculations to express the coefficients c_i through 3 parameters $\kappa_1,\ \kappa_2$, and κ_3 by

$$(c_1, c_2, c_3, c_4) = (\sin\kappa_1, \cos\kappa_1 \sin\kappa_2, \cos\kappa_1 \cos\kappa_2 \sin\kappa_3, \cos\kappa_1 \cos\kappa_2 \cos\kappa_3). \tag{4.16}$$

For the state (4.14) we can obtain an analytical solution for the maximal BI violation and optimal detector configurations in the presence of decoherence, as follows. Now in Eq. (4.8) the elements $\rho^0_{ij} = c_i c_j$ are real and we obtain from Eq. (3.2) the matrix

$$\mathsf{T} = \begin{pmatrix} 2\lambda_a\lambda_b(\rho^0_{23} + \rho^0_{14}) & 0 & 2\lambda_a[\rho^0_{13} + (1-2\gamma_b)\rho^0_{24}] \\ 0 & 2\lambda_a\lambda_b(\rho^0_{23} - \rho^0_{14}) & 0 \\ 2\lambda_b[\rho^0_{12} + (1-2\gamma_a)\rho^0_{34}] & 0 & 1 - 2\gamma_b\rho^0_{22} - 2\gamma_a\rho^0_{33} - 2d\rho^0_{44} \end{pmatrix}, \tag{4.17}$$

where $d = \gamma_a + \gamma_b - 2\gamma_a\gamma_b$ (note that $0 \le d \le 1$). In the matrix T (4.17) only the xz and zx off-diagonal elements are nonvanishing. This allows us to obtain an analytical solution for S_+ and the optimal configurations, using the formalism of Sect. 3, as follows. From Eq. (4.17) we obtain that the nonzero elements of $\mathsf{U} = \mathsf{T}^T\mathsf{T}$ equal

$$\begin{aligned} \mathsf{U}_{xx} &= 4\lambda_b^2\{\lambda_a^2(\rho^0_{14} + \rho^0_{23})^2 + [\rho^0_{12} + (1-2\gamma_a)\rho^0_{34}]^2\}, \\ \mathsf{U}_{yy} &= 4\lambda_a^2\lambda_b^2(\rho^0_{14} - \rho^0_{23})^2, \\ \mathsf{U}_{zz} &= 4\lambda_a^2[\rho^0_{13} + (1-2\gamma_b)\rho^0_{24}]^2 + g^2, \\ \mathsf{U}_{xz} &= \mathsf{U}_{zx} = 4\lambda_a^2\lambda_b(\rho^0_{14} + \rho^0_{23})[\rho^0_{13} + (1-2\gamma_b)\rho^0_{24}] \\ &\quad + 2\lambda_b[\rho^0_{12} + (1-2\gamma_a)\rho^0_{34}]g, \end{aligned} \tag{4.18}$$

where $g = 1 - 2\gamma_b\rho^0_{22} - 2\gamma_a\rho^0_{33} - 2d\rho^0_{44}$.

When $\mathsf{U}_{xz} = \mathsf{U}_{zx} \neq 0$, it is easy to see that the eigenvalues of U are

$$u_y = \mathsf{U}_{yy}, \quad u_\pm = \frac{\mathsf{U}_{xx} + \mathsf{U}_{zz}}{2} \pm \sqrt{\frac{(\mathsf{U}_{xx} - \mathsf{U}_{zz})^2}{4} + \mathsf{U}_{xz}^2}, \tag{4.19}$$

the corresponding eigenvectors being

$$\mathbf{c}_y = \mathbf{y}, \quad \mathbf{c}_\pm = [(u_\pm - \mathsf{U}_{xx})^2 + \mathsf{U}_{xz}^2]^{-1/2}(\mathsf{U}_{xz}, 0, u_\pm - \mathsf{U}_{xx}). \tag{4.20}$$

Thus, we obtain that

$$u_1 = u_+, \quad u_2 = \max\{u_-, \mathsf{U}_{yy}\}, \tag{4.21}$$

which implies two cases,

$$\mathbf{c}_1 = \mathbf{c}_+, \quad \mathbf{c}_2 = \mathbf{c}_- \quad \text{if } u_2 = u_- > \mathsf{U}_{yy}, \tag{4.22}$$

$$\mathbf{c}_1 = \mathbf{c}_+, \quad \mathbf{c}_2 = \mathbf{y} \quad \text{if } u_2 = \mathsf{U}_{yy} > u_-. \tag{4.23}$$

Equations (3.11), (3.18), and (4.17)–(4.23) together with Eqs. (3.22)–(3.24) [or (3.28), (3.32), and (3.35)] provide S_+ and the optimal detector configurations for the state (4.14).

In particular, in the case (4.22) $\mathbf{c}_1$, $\mathbf{c}_2$, $\mathbf{e}_1$, and $\mathbf{e}_2$ are located in the xz plane [see Eqs. (3.18), (4.17), and (4.20)], i.e., all optimal detector axes lie in the xz plane. In contrast, in the case (4.23) $\mathbf{c}_1$ and $\mathbf{e}_1$ are in the xz plane, whereas $\mathbf{c}_2 = \mathbf{y}$ and $\mathbf{e}_2$ equals $\mathbf{y}$ or $-\mathbf{y}$, i.e., the optimal detector axes for the two qubits lie in two respective planes passing through the $\mathbf{y}$ axis.

When U is diagonal, i.e., $\mathsf{U}_{xz} = \mathsf{U}_{zx} = 0$ in Eq. (4.18), the treatment is straightforward. In particular, the case, when U and T are diagonal and $\mathsf{U}_{xx} = \mathsf{U}_{yy}$, was discussed in Sect. 3.5.

We use the above analytical solution to obtain $S_{\max}$ and the corresponding optimal state, by maximizing S_+ numerically over the 3 parameters κ_1, κ_2, and κ_3 in Eq. (4.16). This procedure is significantly faster than the numerical method described in Sect. 4.2. Before the discussion of the results of numerical calculations in Sect. 4.5, we consider important cases which admit simple analytical solutions.

4.4 Analytical solutions for special cases

Here we consider cases allowing for relatively simple analytical solutions.

4.4.1 Horizontal optimal configurations

An especially simple solution is obtained when the optimal observation axes lie in the xy (horizontal) plane. Then Eqs. (4.11) and (4.13) with $a_z = 0$ yield $\mathscr{B}_d = \lambda_a\lambda_b\mathscr{B}$, and hence $S = \lambda_a\lambda_b S_0$, where $S_0 = \mathrm{Tr}\,(\mathscr{B}\rho_0)$ is obtained in the absence of decoherence (Sect. 2). As a result, the value of S maximized over all states and horizontal observation directions is

$$S_+ = S_h \equiv 2\sqrt{2}\lambda_a\lambda_b. \tag{4.24}$$

This value is obtained only for the maximally entangled states which have horizontal optimal detector configurations in the ideal case, as, e.g., the states $|\Psi_+\rangle$ and $|\Phi_+\rangle$ discussed in Sect. 3.5. All such states are given by the expressions

$$|\Psi\rangle = (|01\rangle + e^{i\alpha}|10\rangle)/\sqrt{2}, \tag{4.25}$$

$$|\Phi\rangle = (|00\rangle + e^{i\alpha}|11\rangle)/\sqrt{2}. \tag{4.26}$$

Indeed, taking into account that S is invariant under identical rotations of qubits and detectors, Eq. (2.7), and that all maximally entangled states are related by a rotation of one of the qubits (cf. Sect. 3.4.1), we obtain that all maximally entangled states with horizontal optimal configurations result from the state $|\Psi_+\rangle$ (or $|\Phi_+\rangle$) on applying to one of the qubits an arbitrary rotation around the z axis and/or a π rotation around the x axis, since only such rotations do not take the detector axes out of the horizontal plane. All the resulting states are given by Eqs. (4.25) and (4.26).

The states (4.25) and (4.26) are special cases of the states (4.27) and (4.28), which are discussed in detail in Sect. 4.4.2. In particular, in Sect. 4.4.2 the validity conditions of Eq. (4.24) are obtained.

4.4.2 Even and odd states

It is of interest to consider maximal violations of the BI for the classes of general complex "odd" and "even" states, respectively ($0 \leq \alpha < 2\pi,\ 0 < \beta < \pi/2$),

$$|\Psi\rangle = \sin\beta|01\rangle + e^{i\alpha}\cos\beta|10\rangle, \tag{4.27}$$

$$|\Phi\rangle = \sin\beta|00\rangle + e^{i\alpha}\cos\beta|11\rangle. \tag{4.28}$$

In particular, the state (4.27) is directly obtainable in experiments with superconducting phase qubits [39,51].

It is sufficient to consider the general positive odd and even states, which are special cases of Eq. (4.14),

$$|\Psi\rangle = \sin\beta|01\rangle + \cos\beta|10\rangle \quad (0 < \beta < \pi/2), \tag{4.29}$$

$$|\Phi\rangle = \sin\beta|00\rangle + \cos\beta|11\rangle \quad (0 < \beta < \pi/2). \tag{4.30}$$

Indeed, the states (4.27) and (4.28) result from Eqs. (4.29) and (4.30), respectively, under the rotation of qubit a around the z axis by the angle α. Hence, the results for S_+ obtained in the present paper for the odd and even states (4.29) and (4.30) hold, respectively, also for the states (4.27) and (4.28) with the same β, the corresponding optimal configurations being modified by the rotation of the detectors for qubit a around the z axis by α [cf. the remark after Eq. (4.15)].

For the general (positive) odd and even states (4.29) and (4.30), respectively, Eq. (4.17) yields

$$\mathsf{T} = \mathrm{diag}(\lambda_a\lambda_b\sin 2\beta, \lambda_a\lambda_b\sin 2\beta, 1-\gamma_+-\gamma_-\cos 2\beta), \tag{4.31}$$

$$\mathsf{T} = \mathrm{diag}(\lambda_a\lambda_b\sin 2\beta, -\lambda_a\lambda_b\sin 2\beta, 1-d-d\cos 2\beta), \tag{4.32}$$

where $\gamma_\pm = \gamma_a \pm \gamma_b$. The discussion in Sect. 3.5) applies to the odd and even states, since Eqs. (4.31) and (4.32) have the form of Eqs. (3.48) and (3.49), respectively, with

$$\tau_x = \lambda_a\lambda_b\sin 2\beta, \tag{4.33}$$

whereas for the general odd states

$$\tau_z = \gamma_+ + \gamma_-\cos 2\beta - 1 \tag{4.34}$$

and for the general even states

$$\tau_z = 1 - d - d\cos 2\beta. \tag{4.35}$$

Now only positive values of τ_z are of interest for the BI violation [see Eq. (3.50)].

For both states we obtain,[5] in view of Eq. (3.51),

$$S_+ = 2\max\left\{\sqrt{2}\lambda_a\lambda_b\sin 2\beta, \sqrt{\lambda_a^2\lambda_b^2\sin^2 2\beta + \tau_z^2}\right\}. \tag{4.36}$$

Correspondingly, the optimal configurations for the general odd and even states (with $\tau_z > 0$) are given in Sects. 3.5.1 and 3.5.2, respectively. These configurations lie in the horizontal (a vertical) plane if τ_z is less (greater) than $\lambda_a\lambda_b\sin 2\beta$.

For comparison, in the absence of decoherence Eqs. (4.33)–(4.35) become

$$\tau_x = \sin 2\beta, \quad \tau_z = 1, \tag{4.37}$$

and hence Eq. (4.36) yields [23,43]

$$S_+ = 2\sqrt{1 + \sin^2 2\beta}. \tag{4.38}$$

Since now $\tau_x \le \tau_z$, the optimal detector configurations for the qubits lie in vertical planes, as described in points *b.* in Sects. 3.5.1 and 3.5.2. For $\beta = \pi/4$ the states (4.29) and (4.30) are maximally entangled, and the BI violation is maximal, $S_+ = S_{\max} = 2\sqrt{2}$; then optimal configurations lie both in vertical and horizontal planes [32] (points *c.* in Sects. 3.5.1 and 3.5.2).

In contrast to the ideal case, in the presence of decoherence $S_{\max}$ is not necessarily obtained for a maximally entangled state. It is still of interest to consider S_+ for the maximally entangled odd and even states ($\beta = \pi/4$), i.e., $|\Psi_+\rangle$ and $|\Phi_+\rangle$, respectively. For $|\Psi_+\rangle$ and $|\Phi_+\rangle$ Eq. (4.36) with $\beta = \pi/4$ becomes, respectively,

$$S_+ = S_+^{\Psi} = 2[\lambda_a^2\lambda_b^2 + \max\{\lambda_a^2\lambda_b^2, (\gamma_+ - 1)^2\}]^{1/2}, \tag{4.39}$$

$$S_+ = S_+^{\Phi} = 2[\lambda_a^2\lambda_b^2 + \max\{\lambda_a^2\lambda_b^2, (1 - d)^2\}]^{1/2}. \tag{4.40}$$

When the first term in the braces in Eqs. (4.39) and (4.40) is greater than the second term, Eqs. (4.39) and (4.40) reduce to Eq. (4.24). One can show that generally $1 - d \ge |\gamma_+ - 1|$, the equality here being for $\gamma_a = \gamma_b$ equal to 1 or 0. This yields that $S_+^{\Phi} \ge S_+^{\Psi}$ when the second term in the braces in Eqs. (4.39) and (4.40) is greater than the first term. Hence, in the presence of decoherence, the BI violation for $|\Phi_+\rangle$ is generally greater than for $|\Psi_+\rangle$. This means that the BI violation duration τ_B, defined by $S_+(t = \tau_B) = 2$, is generally greater for $|\Phi_+\rangle$ than for $|\Psi_+\rangle$.

[5] For the general odd state, Eq. (4.36) is a special case for the zero temperature of the result in [33].

Consider now the maximal BI violations for the classes of the general even and odd states. To this end, S_+ in Eq. (4.36) should be maximized with respect to β. This yields for the optimal odd state (4.29)

$$S_+ = 2\lambda_a\lambda_b[1 + \max\{1, (\gamma_+ - 1)^2/(\lambda_a^2\lambda_b^2 - \gamma_-^2)\}]^{1/2} \quad \text{if } \lambda_a^2\lambda_b^2 > d_1, \tag{4.41a}$$

$$S_+ = 2\max\{\sqrt{2}\lambda_a\lambda_b, d_2\} \quad \text{if } \lambda_a^2\lambda_b^2 \leq d_1, \tag{4.41b}$$

where $d_1 = \gamma_-^2 + |\gamma_-|(\gamma_+ - 1) \leq 1$ and $d_2 = |\gamma_+ + |\gamma_-| - 1| \leq 1$, and for the optimal even state (4.30)

$$S_+ = 2\lambda_a\lambda_b\left[1 + \max\left\{1, \frac{(1-d)^2}{\lambda_a^2\lambda_b^2 - d^2}\right\}\right]^{1/2} \quad \text{if } \lambda_a^2\lambda_b^2 > d, \tag{4.42a}$$

$$S_+ = 2 \quad \text{if } \lambda_a^2\lambda_b^2 \leq d. \tag{4.42b}$$

Equations (4.41a) and (4.42a), in contrast to Eqs. (4.41b) and (4.42b), can describe a violation of the BI. When the first term in the braces in Eq. (4.41a) or (4.42a) is greater than the second term, the case (4.24) is realized and the corresponding state is maximally entangled ($\beta = \pi/4$). In the opposite case, the optimal odd and even states generally are not maximally entangled, being characterized by the following values of β, respectively,

$$\beta = \arccos[\gamma_-(\gamma_+ - 1)/(\lambda_a^2\lambda_b^2 - \gamma_-^2)]/2, \tag{4.43}$$

$$\beta = \pi/2 - \arccos[(d - d^2)/(\lambda_a^2\lambda_b^2 - d^2)]/2. \tag{4.44}$$

Note that Eq. (4.41b), with the second term greater than the first term, and Eq. (4.42b) are obtained for a nonentangled initial state: $|10\rangle$ if $T_1^a < T_1^b$ or $|10\rangle$ if $T_1^a > T_1^b$ for Eq. (4.41b) and $|00\rangle$ for Eq. (4.42b).

Numerical calculations show that the maximal BI violation in the optimal even state is greater than or equal to that obtained in the optimal odd state. The differences in S_+ for the optimal even and odd states can appear only in the case when the detectors are in a vertical plane. In this case the optimal states are generally nonmaximally entangled. The reason for this is as follows. While for horizontal detector configurations $S = \lambda_a\lambda_b S_0$ depends only on the dephasing parameters $\lambda_{a,b}$ (see Sect. 4.4.1), S is sensitive to energy relaxation when detectors axes do not lie in the horizontal plane. As a result, for instance, in the optimal even state the amplitude of $|11\rangle$ is less than the amplitude of $|00\rangle$, since this bias reduces spontaneous decay and hence diminishes the detrimental effect of energy relaxation on the BI violation. By the same reason, in the optimal odd state the amplitude of the excited qubit with a smaller γ_k (shorter T_1^k) is reduced. Note, however, a difference between optimal even and odd states. For example, in the case $\gamma_a = \gamma_b$ the optimal odd state, in contrast to the optimal even state, is maximally entangled, since no relaxation reduction can be achieved in a nonmaximally entangled odd state.

4.5 Numerical results and discussion

4.5.1 Pure dephasing

First, let us discuss the case of the absence of energy relaxation, $\gamma_a = \gamma_b = 1$, when decoherence occurs due to pure dephasing. Our calculations show that now both the odd and even Bell states, $|\Psi_+\rangle$ and $|\Phi_+\rangle$, are optimal states providing $S_{\max}$. In this case $\gamma_+ = 2$, $\gamma_- = d = d_1 = 0$, and both Eqs. (4.41) and (4.42) yield [10,47,54]

$$S_{\max} = 2\sqrt{1 + \lambda_a^2 \lambda_b^2}. \tag{4.45}$$

Thus, now the BI can be violated for any level of decoherence, and hence there is no Bell nonlocality sudden death now. The value (4.45) is achieved for the observation axes lying in a vertical plane [47]. The detector orientations for the odd and even Bell states are described in points *b.* in Sects. 3.5.1 and 3.5.2, respectively, taking into account that now $\tau_x = \lambda_a \lambda_b$ and $\tau_z = 1$ for both states. Note that the states (4.27) and (4.28) are also optimal. However, not all maximally entangled states are optimal now [10,54], since S is generally non-invariant with respect to local transformations (see the last paragraph in Sect. 4.1).

4.5.2 Identical decoherence of the qubits

Next, consider the case of identical decoherence for the qubits of a pair. Now

$$\gamma_a = \gamma_b = \gamma, \;\; \lambda_a = \lambda_b = \lambda, \;\; d = 2\gamma(1-\gamma), \;\; \gamma_+ = 2\gamma, \tag{4.46}$$

$\gamma_- = d_1 = 0$, and $\mu_a = \mu_b = \mu$. The numerical calculations show that in this case the maximal S can be always obtained with the even state (4.30), i.e., $S_{\max}$ is given by Eq. (4.42) with the account of Eq. (4.46),

$$S_{\max} = 2\lambda^2 \left[1 + \max\left\{ 1, \frac{(1-d)^2}{\lambda^4 - d^2} \right\} \right]^{1/2} \quad \text{if } \lambda^4 > d, \tag{4.47a}$$

$$S_{\max} = 2 \quad \text{if } \lambda^4 \le d. \tag{4.47b}$$

Now the optimal odd state is the Bell state $|\Psi_+\rangle$, so that Eq. (4.41) reduces to Eq. (4.39), which becomes now

$$S_+ = S_+^{\Psi} = 2\sqrt{\lambda^4 + \max\{\lambda^4, (2\gamma - 1)^2\}}. \tag{4.48}$$

Figure 2 shows the dependence of S_+ on γ with $\mu = 1$ (no pure dephasing) and $\mu = 0.9$ for the even state (when $S_+ = S_{\max}$) and the odd state $|\Psi_+\rangle$. Note that the straight segments in Fig. 2 (in particular, both plots for the odd state given by dashed lines) correspond to the case of horizontal optimal configurations where $S_+ = S_h = 2\sqrt{2}\lambda^2$ [Eq. (4.24)]. Equation (4.47a) and Fig. 2 imply that the violation of the BI is possible only for $\gamma > 2/3$, this limit being approached for the

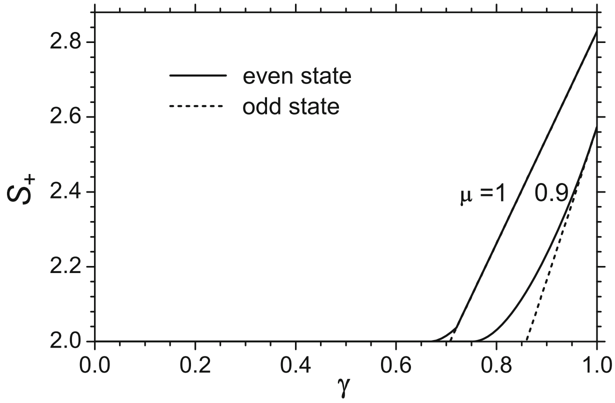

Fig. 2 S_+ versus the relaxation parameter γ for $\mu = 1$ (no pure dephasing) and $\mu = 0.9$, where $\mu = \lambda/\sqrt{\gamma}$. *Solid lines* $S_+ = S_{\max}$ (4.47) for the even state (4.30), *dashed lines* Eq. (4.48) for the odd Bell state $|\Psi_+\rangle$ (2.14)

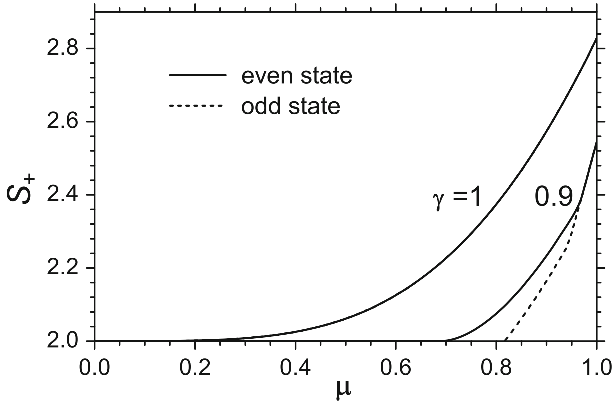

Fig. 3 S_+ versus the pure dephasing parameter μ for $\gamma = 1$ (no decay) and $\gamma = 0.9$. *Solid lines* $S_+ = S_{\max}$ (4.47) with the even state (4.30), *dashed lines* Eq. (4.48) for the odd state $|\Psi_+\rangle$ (2.14)

vanishing pure dephasing ($\mu = 1$). As a result, for a given value of T_1, the maximal BI violation duration τ_B is obtained for the even state when $\mu = 1$, being given by $\gamma = e^{-\tau_B/T_1} = 2/3$ or $\tau_B = T_1 \ln 1.5 \approx 0.405T_1$. For comparison, we mention that in the case $\mu = 1$ the odd state yields $S_+ = S_h = 2\sqrt{2}\gamma$, so that the BI can be violated only for $\gamma > 1/\sqrt{2} \approx 0.707$. This corresponds to the longest τ_B for the odd state with a given T_1 equal to [31,33] $\tau_B = T_1 \ln 2/2 \approx 0.347T_1$. Note that, in contrast to [31], we obtain different values of τ_B for the even and odd states.

Figure 3 shows the dependence of S_+ on the pure dephasing parameter $\mu = \lambda/\sqrt{\gamma}$. In the absence of energy relaxation ($\gamma = 1$) the plots for the odd and even states coincide and are given by Eq. (4.45), $S_+ = S_{\max} = \sqrt{1+\mu^4} = \sqrt{1+\lambda^4}$. In this case violations of the BI can be achieved for any degree of pure dephasing.

Figure 4 is a contour plot of S_+ as a function of γ and μ. The boundary of the region of the BI violation is shown by the solid line with $S_+ = S_{\max} = 2$. This boundary is

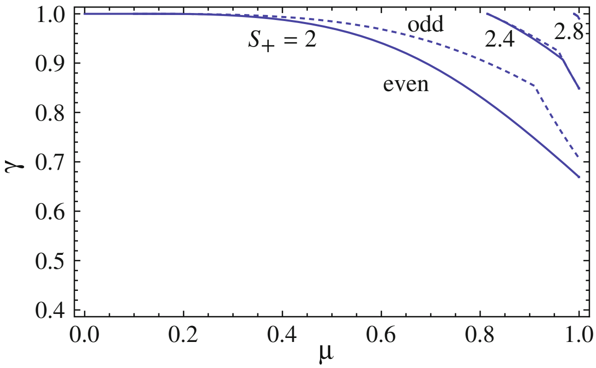

Fig. 4 Contour plot of the maximum S_+ of S versus γ and μ. *Solid lines* the even state (4.30) ($S_+ = S_{\max}$), *dashed lines* the odd state $|\Psi_+\rangle$

obtained when the second term dominates in the braces in Eq. (4.47a). The kinks on the curves in Figs. 2, 3, and 4 correspond to a change of the dominating term in the braces in Eqs. (4.47a) and (4.48). Figures 2, 3, and 4 show that S_+ for the odd state is generally lower than $S_{\max}$, which results in more stringent conditions on the decoherence parameters required for the BI violation than for the even state. The difference is significant when $S_+ - 2$ is small. However, for $S_+ \geq 2.4$ there is practically no difference in the values of S_+ for the odd and even states.

4.5.3 No decoherence in one qubit

Consider the extreme case of nonequal decoherence of the qubits, i.e., the case when decoherence is absent in one of the qubits, e.g., in qubit b. Now $\gamma_b = \lambda_b = 1$, $\gamma_+ = 1+\gamma_a$, $d = d_1 = -\gamma_- = 1-\gamma_a$, $d_2 = 1$, and hence Eqs. (4.41) and (4.42) coincide, i.e., both odd and even states give the same maximal BI violation S_+. This S_+ is maximally possible, $S_+ = S_{\max}$, as shown by our numerical calculations, so that

$$S_{\max} = 2\lambda_a\sqrt{\max\left\{2, \frac{\lambda_a^2 + 2\gamma_a - 1}{\lambda_a^2 - (1-\gamma_a)^2}\right\}} \text{ if } \lambda_a^2 > 1 - \gamma_a, \tag{4.49a}$$

$$S_{\max} = 2 \quad \text{if } \lambda_a^2 \leq 1 - \gamma_a. \tag{4.49b}$$

The optimal value of β corresponding to Eq. (4.49a) follows from Eq. (4.43) or (4.44) to be

$$\beta = \pi/2 - \arccos\{(\gamma_a - \gamma_a^2)/[\lambda_a^2 - (1-\gamma_a)^2]\}/2. \tag{4.50}$$

Since qubit b is not affected by decoherence, S_+ is invariant with respect to arbitrary rotations of qubit b. Therefore, all states obtained from the optimal odd (or even) state by rotations of qubit b are optimal. [This explains why the states (4.29) and (4.30) yield the same results: these states are related by the unitary transformation σ_x^b of the qubit b.] Moreover, since maximally entangled states transform to each other by

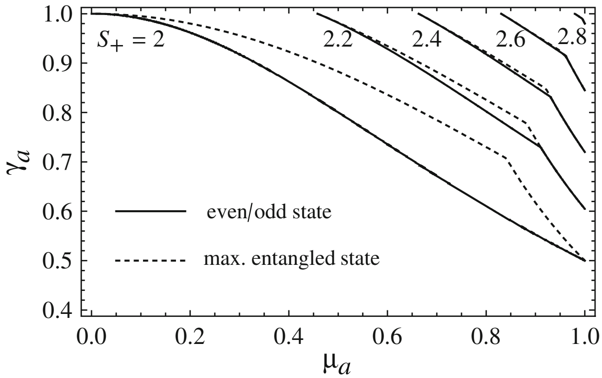

Fig. 5 Contour plot of the maximum S_+ of S versus γ_a and μ_a. *Solid lines* $S_+ = S_{\max}$ (4.49) for the even state (4.30) and the odd state (4.29), *dashed lines* Eq. (4.51) for a maximally entangled state

a rotation of one qubit [56], S_+ is the same for all maximally entangled states [cf. Eq. (4.39) or (4.40)], being given by

$$S_+ = \begin{cases} 2\sqrt{2}\lambda_a, & T_1^a \le T_2^a, \\ 2\sqrt{\lambda_a^2 + \gamma_a^2}, & T_1^a \ge T_2^a. \end{cases} \tag{4.51}$$

Figure 5 shows the contour plot of S_+ versus γ_a and μ_a for the even and odd states which produce $S_+ = S_{\max}$ (the solid lines) and for any maximally entangled state (the dashed lines). Equation (4.49) and Fig. 5 imply that now the BI violation is possible for $\gamma_a > 0.5$, this limit being approached in the absence of proper dephasing ($\mu_a = 1$). Hence, in particular, for $\mu_a = 1$ the BI violation duration maximized over all states is given by $\tau_B = T_1 \ln 2 \approx 0.693 T_1$. Equations (4.49a) and (4.51) imply that the BI violation for maximally entangled states is maximal ($S_+ = S_{\max}$) when there is no energy relaxation ($\gamma_a = 1$) or when the first term in the braces in Eq. (4.49a) is dominating (see Fig. 5); the latter occurs for a sufficiently weak pure dephasing, $\mu > (2\sqrt{2} - 2)^{1/2} \approx 0.910$, when $\gamma_2 < \gamma_a < \gamma_1$ where $\gamma_{1,2} = [2 + \mu^2 \pm \sqrt{(2+\mu^2)^2 - 8}]/4$. Note that maximally entangled states produce practically the same BI violation as the optimal states for $S_+ \ge 2.4$.

4.5.4 General case

In the general case when the decoherence parameters for the two qubits are different, the maximum of the BI violation can be obtained in a state of the form (4.14), as discussed in Sect. 4.3. We performed several hundred calculations of S_+ for the states (4.14) and (4.30) with random values of the four parameters γ_k and μ_k ($k = a, b$) from the interval [0.8, 1]. In our calculations the maximal violation of the BI inequality resulted from the even state (4.30) in about 70% of the cases. In the cases, where the even state did not yield the maximal S, there were various optimal states, which included both general maximally entangled states (2.16) and nonmaximally entangled states. However, the difference between $S_{\max}$ and S_+ due to the optimal even state was less than 0.1.

Thus, there can be several approaches to obtain $S_{\max}$ and the optimal observation conditions for given decoherence parameters, In the decreasing order of the degree of complexity and accuracy, such approaches are as follows: (a) One can use the exact numerical approach of Sect. 4.3, which provides $S_{\max}$, the optimal state, and the optimal detector configurations. (b) A simpler approach is to use the optimal even state [Eqs. (4.30) and (4.44)], which provides rather accurate, if not exact, result (4.42), as discussed above. (c) The analytical formulas (4.41) and (4.43) for the optimal odd state can be used, if, e.g., in the experiment the odd state is realized more conveniently than other entangled states, as is the case for experiments with superconducting phase qubits. (d) An even simpler approach is to use the Bell state $|\Psi_+\rangle$ or $|\Phi_+\rangle$ [see Eqs. (4.39) and (4.40)]. However, if one requires a significant degree of the BI violation, say, $S_+ \geq 2.4$ (which may be needed in the presence of other experimental errors), any of the approaches (b)–(d) yields values of S_+ which are very close to $S_{\max}$ (see Figs. 4, 5).

5 Decoherence and measurement errors

In the previous sections we assumed that measurements are ideal. Here we take into account the possibility that measurements of the qubits are performed with local (independent) errors. Effects of local errors were studied elsewhere [20,32]. In this section we discuss combined effects of local errors and local decoherence. The present case is rather involved, since it includes complications due to both decoherence and errors. Here we discuss only the general approach to the problem, whereas a detailed analysis is out of the scope of the present paper (see also [32]).

5.1 Bell inequality in the presence of measurement errors

As in [32], we describe measurement errors by the fidelity matrix $\{F^k_{im}\}$, where F^k_{im} is the probability to find qubit k in state $|i\rangle$ when it is actually in state $|m\rangle$. Since $F^k_{0m} + F^k_{1m} = 1$, there are two independent error parameters per qubit, e.g., $F^k_0 = F^k_{00}$ and $F^k_1 = F^k_{11}$, the measurement fidelities for the states $|0\rangle$ and $|1\rangle$, respectively. As shown in [32], in the presence of local measurement errors the BI has the form (2.2), where now

$$S = \mathrm{Tr}\,(\tilde{\mathscr{B}}\rho) \tag{5.1}$$

and the error modified Bell operator is given by

$$\tilde{\mathscr{B}} = \tilde{A}\tilde{B} - \tilde{A}\tilde{B}' + \tilde{A}'\tilde{B} + \tilde{A}'\tilde{B}'. \tag{5.2}$$

Here, e.g.,

$$\tilde{A} = \xi^a_- + \xi^a_+ \mathbf{a}\cdot\boldsymbol{\sigma}_a, \quad \tilde{B} = \xi^b_- + \xi^b_+ \mathbf{b}\cdot\boldsymbol{\sigma}_b, \tag{5.3}$$

where

$$\xi_+^k = F_0^k + F_1^k - 1, \quad \xi_-^k = F_1^k - F_0^k, \tag{5.4}$$

$\tilde{A}'$ and $\tilde{B}'$ following from $\tilde{A}$ and $\tilde{B}$ in Eq. (5.3) on the replacement of **a** and **b** by **a**$'$ and **b**$'$, respectively.

Consider properties of S which can be helpful in calculations [32]. The property (i) of S (Sect. 2.1) holds also in the presence of errors. However, the properties (ii) and (iii) generally do not hold now. As a result, in the case with errors, the maximal and minimal values of S for a given state are generally not equal by the magnitude, $S_+ \neq |S_-|$, so that the maximum BI violation for a given state is determined by $\max\{S_+, |S_-|\}$. Note, however, the relations which follow from Eqs. (5.1)–(5.4),

$$S \to -S \;\text{ if }\; \mathbf{a} \to -\mathbf{a},\; \mathbf{a}' \to -\mathbf{a}',\; F_0^a \leftrightarrow F_1^a; \tag{5.5a}$$

$$S \to -S \;\text{ if }\; \mathbf{b} \to -\mathbf{b},\; \mathbf{b}' \to -\mathbf{b}',\; F_0^b \leftrightarrow F_1^b. \tag{5.5b}$$

Equations (5.5) imply that $S_+ = |S_-|$ if the two measurement fidelities are equal, at least, for one qubit:

$$F_0^a = F_1^a \quad \text{or} \quad F_0^b = F_1^b. \tag{5.6}$$

5.2 Modified Bell operator for decoherence and errors

In the presence of decoherence and errors one should substitute Eq. (4.1) into Eq. (5.1). It is useful to recast the resulting expression as

$$S = \mathrm{Tr}\,(\hat{\mathscr{B}}\rho_0) \tag{5.7}$$

where the Bell operator modified by errors and decoherence is

$$\hat{\mathscr{B}} = (\mathscr{L}_a^* \otimes \mathscr{L}_b^*)(\tilde{\mathscr{B}}) = \hat{A}\hat{B} - \hat{A}\hat{B}' + \hat{A}'\hat{B} + \hat{A}'\hat{B}'. \tag{5.8}$$

It is straightforward to show that [cf. Eq. (4.13)]

$$\hat{A} = \xi_-^a + \xi_+^a(1-\gamma_a)a_z + \xi_+^a \mathbf{q}_a \cdot \boldsymbol{\sigma}_a, \tag{5.9}$$

whereas the operators $\hat{A}'$, $\hat{B}$, and $\hat{B}'$ are given by Eq. (5.9), where **a** is replaced by **a**$'$, **b**, and **b**$'$, respectively.

In the special case when for each qubit the measurement fidelities for the two states are equal,

$$F_0^a = F_1^a = F_a, \;\; F_0^b = F_1^b = F_b, \tag{5.10}$$

Equation (5.8) yields $\hat{\mathscr{B}} = (2F_a - 1)(2F_b - 1)\mathscr{B}_d$ and hence

$$S = (2F_a - 1)(2F_b - 1)S_d, \tag{5.11}$$

where S_d is the value of S obtained in the presence of decoherence but in the absence of measurement errors. This case can be analyzed, as discussed in Sect. 4.

5.3 Qubit-swap symmetry

In the presence of the errors, the theory of Sect. 3 is not applicable. The reason for this is that S in Eq. (5.1) depends on ρ not only through the matrix T, as in Eq. (3.3), but also through the vectors $\mathbf{r}_a$ and $\mathbf{r}_b$ in Eq. (3.1). Actually, now there are, in a sense, much less optimal configurations for a given state than for the case of ideal measurements [32]. Anyhow, there is always, at least, one optimal configuration maximizing $|S|$. However, in the case of equal measurement errors for the two qubits,

$$F_0^a = F_0^b, \quad F_1^a = F_1^b, \tag{5.12}$$

there exists an important class of states for which there are, at least, two optimal configurations. This class consists of symmetric states and the states equivalent to symmetric states up to local unitary transformations.

We call a state symmetric if it is symmetric with respect to a qubit swap, i.e., it is not changed under a swap of the qubit labels in Eq. (3.1). In other words, the state is symmetric if in Eq. (3.1)

$$\mathsf{T}^T = \mathsf{T}, \quad \mathbf{r}_a = \mathbf{r}_b. \tag{5.13}$$

Taking into account that in the case (5.12) the Bell operator (5.2) is invariant when simultaneously the qubit labels are swapped and the substitution

$$(\mathbf{a}, \mathbf{a}', \mathbf{b}, \mathbf{b}') \to (\mathbf{b}', \mathbf{b}, \mathbf{a}', \mathbf{a}) \tag{5.14}$$

is made, we obtain that for a symmetric state, S in Eq. (5.1) is invariant under the substitution (5.14). Thus, in the case of equivalent errors (5.12) and a symmetric state, there exist, at least, two optimal configurations, these configurations being related by the substitution (5.14).

Moreover, for any state obtained from a symmetric state by a local transformation (2.7a) there exist, at least, two optimal configurations. The relation between two configurations providing the same S, and hence between the optimal configurations, is given by Eq. (5.14), where $\mathbf{a}$, $\mathbf{a}'$, $\mathbf{b}$, and $\mathbf{b}'$ are replaced, respectively, by $\mathsf{R}_a^T\mathbf{a}$, $\mathsf{R}_a^T\mathbf{a}'$, $\mathsf{R}_b^T\mathbf{b}$, and $\mathsf{R}_b^T\mathbf{b}'$ [cf. Eq. (2.7b)]; thus, the relation is

$$(\mathbf{a}, \mathbf{a}', \mathbf{b}, \mathbf{b}') \to (\mathsf{R}_{ab}\,\mathbf{b}', \mathsf{R}_{ab}\,\mathbf{b}, \mathsf{R}_{ab}^T\mathbf{a}', \mathsf{R}_{ab}^T\mathbf{a}), \quad \mathsf{R}_{ab} = \mathsf{R}_a\mathsf{R}_b^T. \tag{5.15}$$

An example of a state symmetric with respect to a qubit swap is the even state (4.30). Indeed, this state has a diagonal T (see Sect. 4.4.2) and $\mathbf{r}_a = \mathbf{r}_b = -\mathbf{z}\cos 2\beta$. Any pure state can be reduced to the form (4.30) by local rotations of the qubits, since Eq. (4.30) is the Schmidt decomposition [42] for pure two-qubit states. Thus, for any pure state there are, at least, two optimal detector configurations providing maximal BI violations in the presence of equivalent errors.

Generally, mixed states resulting from pure states due to decoherence cannot be made symmetric by local rotations. However, there are notable exceptions, as follows. Mixed states resulting from the even state (4.30) or an odd Bell state (2.14) due to decoherence with $\gamma_a = \gamma_b = \gamma$ are symmetric, since then T is diagonal [Eqs. (4.32), (4.31)] and it is easy to show that $\mathbf{r}_a = \mathbf{r}_b = \mathbf{z}(1-2\gamma\cos^2\beta)$ and $\mathbf{r}_a = \mathbf{r}_b = \mathbf{z}(1-\gamma)$, respectively. Furthermore, a mixed state resulting from the odd state (4.29) due to pure dephasing is equivalent to a symmetric state up to a rotation of one of the qubits by π around the x axis. In contrast, a state resulting from a nonmaximally entangled odd state due to energy relaxation (and perhaps pure dephasing) cannot be made symmetric by local rotations, since then $|\mathbf{r}_a| \neq |\mathbf{r}_b|$.

5.4 Discussion

There is no analytical solution in the presence of errors [20,32]. Moreover, the present case involves an eight-dimensional parameter space (there are two decoherence parameters and two measurement fidelities for each qubit), which additionally complicates the analysis.

Similarly to Sect. 4.2, the modified Bell operator $\hat{\mathscr{B}}$ (5.8) can be used for numerical calculations, since for given decoherence and error parameters the maximum (minimum) value of S equals the maximum (minimum) of the greatest (smallest) eigenvalue of $\hat{\mathscr{B}}$ over the detector directions, the optimal state being given by the corresponding eigenvector. Now, as in Sect. 4, S is invariant to rotations of the qubits and detectors around the z axis, which allows one to reduce the number of the fitting parameters from eight to six by setting, say, $a_y = b_y = 0$. This number cannot be further reduced, since now point (i) in Sect. 4.2 is not applicable.

This computation procedure is relatively slow. It produces generally different optimal states for different values of the parameters. An approach which is faster and more relevant for most experiments is to consider the BI violation for a specific initial state ρ_0, e.g., the odd or even state [Eqs. (4.29) and (4.30), respectively]. In this case an expression for S resulting from Eq. (5.7) is varied over the detector directions and perhaps the state parameters [e.g., β in Eqs. (4.29) and (4.30)] in order to obtain S_+ and S_-.

Note that in the cases of the odd and even states the number of the detector parameters can be reduced from eight to seven, as follows. When the initial state is odd (even), for the measured state ρ (4.8) which underwent decoherence, the only nonvanishing off-diagonal elements are $\rho_{23} = \rho_{32}$ ($\rho_{14} = \rho_{41}$). As a result, for the odd (even) initial state, the density matrix ρ is invariant under a rotation of qubits a and b around the z axis by an arbitrary angle α (angles α and $-\alpha$, respectively). Because of the invariance of S under identical rotations of the qubits and detectors, Eq. (2.7), one can reduce the number of the detector parameters by moving, say, $\mathbf{a}$ into the xz plane, i.e., choosing

$a_y = 0$. A detailed analysis of the case of the odd state, Eq. (4.29), is performed in [32]; the even state can be discussed in a similar way.

6 Conclusions

In the present paper we have considered conditions for maximal violations of the Bell inequality in the presence of decoherence. In addition, combined effects of decoherence and local measurement errors have been discussed.

Since decoherence transforms a pure entangled state into a mixed state, we have begun the consideration from the study of optimal conditions for the violation of the BI (2.2) for a general (pure or mixed) state. We have obtained all detector configurations providing the maximal value of the CHSH parameter S in Eq. (2.2) for an arbitrary state. We have shown that generally the set of all optimal configurations for a given state is characterized by one continuous and one discrete parameters, whereas in special cases it can be characterized by two or three continuous parameters. We have obtained also the symmetry relation for the optimal detector orientations, Eq. (3.40) or (3.41), which follows from the invariance of S with respect to the qubit swap.

Further, we have considered effects of local decoherence on the BI violation. We have used the decoherence superoperator in the operator-sum form, which describes energy relaxation at the zero temperature and arbitrary pure dephasing. We have expressed S as the average over the initial state of the Bell operator modified by decoherence. This operator has been used for numerical calculations in order to obtain the maximal BI violation for any values of the decoherence parameters. We have reduced the number of varied parameters from 8 to 5 and thus significantly accelerated the calculations, using the symmetry of the decoherence model and the fact revealed here (Sect. 3) that the set of optimal configurations for a given state is continuous. Our calculations have allowed us to identify a class of two-qubit pure states (the real states) which provide maximal BI violations for all values of decoherence parameters. We have obtained an analytical solution for this class of states and used it to develop a fast numerical approach for maximizing Bell violations.

We have obtained simple analytical solutions for both optimal and maximally entangled odd and even states. Such states are often used in experiments on the BI violation. In particular, the general odd state is relevant for experiments with superconducting phase qubits. While in the absence of decoherence the optimal detector configurations for the odd and even states are vertical, in the presence of decoherence, they are either vertical or horizontal. We have discussed both the general case of arbitrary decoherence parameters and a number of important special cases. In particular, we have revealed that the even state is optimal in most cases. Our analysis have been illustrated by numerical calculations.

Moreover, the combined effects of local errors and decoherence have been considered. In this case the maximal Bell violation depends on eight parameters. We have derived the Bell operator modified by decoherence and errors and have used it to discuss symmetry properties of S. Numerical approaches in this case have been also outlined.

The present results are applicable to many types of qubits, including, in particular, superconducting qubits. Moreover, the present results have relevance to the ongoing discussion of effects of decoherence on entanglement, a major resource in the field of quantum information.

Acknowledgments I am grateful to A. N. Korotkov for useful discussions and for the encouragement of this work. The work was supported by NSA and DTO under ARO grant W911NF-04-1-0204.

Appendix

A BI violations and entanglement for pure states

Here we obtain the maximal BI violation S_+ and the entanglement measure, the concurrence $\mathscr{C}$, for the state (2.19). Any pure two-qubit state $|\Psi\rangle$ can be written in the Schmidt form [42]

$$|\Psi\rangle = s_1|i_a i_b\rangle + s_2|j_a j_b\rangle. \tag{A.1}$$

Here $s_{1,2} \geq 0$ and $s_1^2 + s_2^2 = 1$, whereas $\{|i_a\rangle, |j_a\rangle\}$ and $\{|i_b\rangle, |j_b\rangle\}$ are orthonormal bases for qubits a and b, respectively. For the state (A.1), we obtain that [23,43] [cf. Eq. (4.38)]

$$S_+ = 2\sqrt{1 + 4s_1^2 s_2^2} \tag{A.2}$$

and [55]

$$\mathscr{C} = 2s_1 s_2. \tag{A.3}$$

Combining Eqs. (A.2) and (A.3) yields Eq. (2.17).

For the state (2.19), the quantities s_1^2 and s_2^2 are [42] eigenvalues of $D_1 = D^T D$, where

$$D = \begin{pmatrix} c_1 & c_2 \\ c_3 & c_4 e^{i\alpha} \end{pmatrix}. \tag{A.4}$$

It is easy to see that the eigenvalues of D_1 are the solutions of the following equation for the variable s^2,

$$(s^2)^2 - s^2 \mathrm{Tr}\, D_1 + \det(D_1) = 0. \tag{A.5}$$

We obtain that $\mathrm{Tr}\, D_1 = 1$ and

$$\det(D_1) = |\det(D)|^2 = |c_1 c_4 e^{i\alpha} - c_2 c_3|^2. \tag{A.6}$$

The solutions of Eq. (A.5) are

$$s_{1,2}^2 = \frac{1 \pm \sqrt{1 - 4\det(D_1)}}{2}. \tag{A.7}$$

Inserting Eq. (A.7) into Eq. (A.3) yields $\mathscr{C} = 2\sqrt{\det(D_1)}$. The latter equality with the account of Eq. (A.6) yields Eq. (2.20).

B Properties of matrix T

Consider some useful properties of the matrix T in Eq. (3.1). Since the eigenvalues of the Hermitian operators $\sigma_m^a \sigma_n^b$ equal ± 1, Eq. (3.2) implies that

$$|\mathsf{T}_{mn}| \leq 1. \tag{B.1}$$

There exists the polar decomposition [42]

$$\mathsf{T} = \mathsf{V}\sqrt{\mathsf{U}}, \tag{B.2}$$

where V is a 3×3 orthogonal matrix, $\mathsf{V}^T\mathsf{V} = I_3$, and $\mathsf{U} = \mathsf{T}^T\mathsf{T}$ is a real symmetric matrix with nonnegative eigenvalues $u_1,\ u_2, u_3 (0 \leq u_3 \leq u_1, u_2)$. V is unique, being given by $\mathsf{V} = \mathsf{T}\mathsf{U}^{-1/2}$, only if $u_3 \neq 0$; this is the most interesting case, as shown below. The determinant of V equals 1 or -1 for $\det(\mathsf{T}) > 0$ and $\det(\mathsf{T}) < 0$, respectively; when $\det(\mathsf{T}) = 0$ (which means that $u_3 = 0$), V can be chosen such that $\det(\mathsf{V}) = 1$.

Under a local unitary transformation $\rho \to (U_a \otimes U_b)\rho(U_a^\dagger \otimes U_b^\dagger)$ Eq. (3.1) changes so that $\mathbf{r}_k \to \mathsf{R}_k\mathbf{r}_k$ and [49]

$$\mathsf{T} \to \mathsf{R}_a\mathsf{T}\mathsf{R}_b^T, \tag{B.3}$$

where $\mathsf{R}_{a,b}$ are defined after Eq. (2.7b). As follows from Eqs. (B.2) and (B.3), with suitable rotations of the qubits, R_a' and R_b', the matrix T can be reduced to one of the two diagonal forms, $\mathsf{T}' = \mathsf{R}_a'\mathsf{T}(\mathsf{R}_b')^T = \pm\sqrt{\mathsf{U}'}$. Here R_b' is such that $\mathsf{U}' = \mathsf{R}_b'\mathsf{U}\,(\mathsf{R}_b')^T$ is diagonal and $\mathsf{R}_a' = \pm\mathsf{R}_b'\mathsf{V}^T$. The plus and minus signs in the above formulas are obtained for $\det(\mathsf{T}) \geq 0$ and $\det(\mathsf{T}) < 0$, respectively [on choosing $\det(\mathsf{V}) = 1$ when $\det(\mathsf{T}) = 0$]. As a consequence, in view of Eq. (B.1), we obtain

$$0 \leq u_3 \leq u_1, u_2 \leq 1. \tag{B.4}$$

Note that an arbitrary two-qubit state reduces to a simpler form by a local unitary transformation which diagonalizes T. Inserting a general diagonal T into Eq. (3.1), we obtain that all states with a diagonal T have the form

$$\rho = \begin{pmatrix} \rho_{11} & \rho_{12} & \rho_{13} & \rho_{14} \\ \rho_{21} & \rho_{22} & \rho_{23} & \rho_{13} \\ \rho_{31} & \rho_{23} & \rho_{33} & \rho_{12} \\ \rho_{14} & \rho_{31} & \rho_{21} & \rho_{44} \end{pmatrix}. \tag{B.5}$$

In the state (B.5) $\rho_{12} = \rho_{34}$ and $\rho_{13} = \rho_{24}$, whereas ρ_{14} and ρ_{23} are real.[4]

For the state (B.5) we obtain from Eq. (3.2) that

$$\mathsf{T} = 2\,\mathrm{diag}(\rho_{23} + \rho_{14}, \rho_{23} - \rho_{14}, 1/2 - \rho_{22} - \rho_{33}). \tag{B.6}$$

Note that this expression is independent of ρ_{12}, ρ_{21}, ρ_{13}, and ρ_{31}.

The states with $\det(\mathsf{T}) \geq 0$ do not violate the BI. To show this, it is sufficient to consider a diagonal $\mathsf{T} = \sqrt{\mathsf{U}}$, since, as mentioned above, such T can be obtained for any state with $\det(\mathsf{T}) \geq 0$ by means of local unitary transformations, which do not change S. A diagonal $\mathsf{T} = \sqrt{\mathsf{U}}$ is given by Eq. (B.6) with nonnegative matrix elements, which implies that $r \equiv \rho_{22} + \rho_{33} \leq 1/2$ and $\rho_{23} \geq |\rho_{14}|$. As follows from Eq. (B.6), $\mathrm{Tr}\,\mathsf{U} = \mathrm{Tr}\,\mathsf{T}^2 = 4\rho_{14}^2 + 4\rho_{23}^2 + (1 - 2r)^2$. For a given r, $\mathrm{Tr}\,\mathsf{U}$ is maximal if ρ_{23} and $|\rho_{14}|$ are maximal under the above constraints, i.e., if $|\rho_{14}| = \rho_{23} = r/2$, which yields $\mathrm{Tr}\,\mathsf{U} \leq 6r^2 - 4r + 1$ $(0 \leq r \leq 1/2)$. This expression achieves the maximum $\mathrm{Tr}\,\mathsf{U} = 1$ for $r = 0$. Thus, in the case $\det(\mathsf{T}) \geq 0$ we have $\mathrm{Tr}\,\mathsf{U} \leq 1$, the value $\mathrm{Tr}\,\mathsf{U} = 1$ being obtained for the states which, with the accuracy to local unitary transformations, have the form $\rho = \mathrm{diag}(\rho_{11}, 0, 0, \rho_{44})$ and hence have $\mathsf{T} = \mathsf{U} = \mathrm{diag}(0, 0, 1)$ [see Eq. (B.6)]. In view of Eq. (3.11), these states yield $S_+ = 2$; they include, in particular, pure nonentangled states.

However, the BI violation implies $\mathrm{Tr}\,\mathsf{U} \geq u_1 + u_2 > 1$. Hence, a necessary condition for the BI violation is $\det(\mathsf{T}) < 0$. As a consequence, in view of Eq. (B.2), for the states violating the BI all u_i do not vanish. Note that in the case $\det(\mathsf{T}) < 0$ Eq. (B.2) can be recast in the form (3.14).

References

1. Alicki, R., Lendi, K.: Quantum Dynamical Semigroups and Applications. Springer, Berlin (1987)
2. Altepeter, J.B., Jeffrey, E.R., Kwiat, P.G.: Phase-compensated ultra-bright source of entangled photons. Opt. Express **13**, 8951–8959 (2005)
3. Ann, K., Jaeger, G.: Generic tripartite Bell nonlocality sudden death under local phase noise. Phys. Lett. A **372**, 6853–6858 (2008)
4. Ansmann, M., Wang, H., Bialczak, R.C., Hofheinz, M., Lucero, E., Neeley, M., O'Connell, A.D., Sank, D., Weides, M., Wenner, J., Cleland, A.N., Martinis, J.M.: Violation of Bell's inequality in Josephson phase qubits. Nature **461**, 504–506 (2009)
5. Aspect, A.: Bell's theorem: the naive view of an experimentalist. In: Bertlmann, R.A., Zeilinger, A. (eds.) Quantum [Un]speakables—From Bell to Quantum Information, pp. 119–153. Springer, Berlin (2002)
6. Aspect, A., Dalibard, J., Roger, G.: Experimental test of Bell inequalities using time-varying analyzers. Phys. Rev. Lett. **49**, 1804–1807 (1982)
7. Aspect, A., Grangier, P., Roger, G.: Experimental tests of realistic local theories via Bell's theorem. Phys. Rev. Lett. **47**, 460–463 (1981)
8. Aspect, A., Grangier, P., Roger, G.: Experimental realization of Einstein–Podolsky–Rosen–Bohm gedankenexperiment—a new violation of Bell inequalities. Phys. Rev. Lett. **49**, 91–94 (1982)
9. Ban, M.: Decoherence of qubit entanglement caused by transient environments. J. Phys. B **40**, 689–696 (2007)
10. Beenakker, C.W.J., Emary, C., Kindermann, M., Velsen, J.L.van : Proposal for production and detection of entangled electron-hole pairs in a degenerate electron gas. Phys. Rev. Lett. **91**, 147,901 (2003)
11. Bell, J.S.: On the Einstein Podolosky Rosen paradox. Physics **1**, 195–200 (1964)
12. Bell, J.S: Introduction to the hidden-variable question. In: d'Espagnat, B. (ed.) Foundations of Quantum Mechanics, pp. 171–181. Academic, New York (1971)

13. Berkley, A.J., Xu, H., Ramos, R.C., Gubrud, M.A., Strauch, F.W., Johnson, P.R., Anderson, J.R., Dragt, A.J., Lobb, C.J., Wellstood, F.C.: Entangled macroscopic quantum states in two superconducting qubits. Science **300**, 1548–1550 (2003)
14. Braunstein, S.L., Mann, A., Revzen, M.: Maximal violation of Bell inequalities for mixed states. Phys. Rev. Lett. **68**, 3259–3261 (1992)
15. Capasso, V., Fortunato, D., Selleri, F.: Sensitive observables of quantum mechanics. Int. J. Theor. Phys. **7**, 319–326 (1973)
16. Cirel'son, B.S.: Quantum generalizations of Bell's-inequality. Lett. Math. Phys. **4**, 93–106 (1980)
17. Claudon, J., Balestro, F., Hekking, F.W.J., Buisson, O.: Coherent oscillations in a superconducting multilevel quantum system. Phys. Rev. Lett. **93**, 187,003 (2004)
18. Clauser, J.F., Horne, M.A., Shimony, A., Holt, R.A.: Proposed experiment to test local hidden-variable theories. Phys. Rev. Lett. **23**, 880–883 (1969)
19. Cohen-Tannoudji, C., Dupont-Roc, J., Grynberg, G.: Atom-Photon Interactions. Wiley, New York (1992)
20. Eberhard, P.H.: Background level and counter efficiencies required for a loophole-free Einstein–Podolsky–Rosen experiment. Phys. Rev. A **47**, R747–R750 (1993)
21. Einstein, A., Podolsky, B., Rosen, N.: Can quantum-mechanical description of physical reality be considered complete?. Phys. Rev. **47**, 777–780 (1935)
22. Ekert, A.K.: Quantum cryptography based on Bell theorem. Phys. Rev. Lett. **67**, 661–663 (1991)
23. Gisin, N.: Bell inequality holds for all non-product states. Phys. Lett. A **154**, 201–202 (1991)
24. Hasegawa, Y., Loidl, R., Badurek, G., Baron, M., Rauch, H.: Violation of a Bell-like inequality in single-neutron interferometry. Nature **425**, 45–48 (2003)
25. Hill, S., Wootters, W.K.: Entanglement of a pair of quantum bits. Phys. Rev. Lett. **78**, 5022–5025 (1997)
26. Hioe, F.T., Eberly, J.H.: N-level coherence vector and higher conservation-laws in quantum optics and quantum-mechanics. Phys. Rev. Lett. **47**, 838–841 (1981)
27. Horodecki, R., Horodecki, P., Horodecki, M.: Violating Bell inequality by mixed spin-1/2 states—necessary and sufficient condition. Phys. Lett. A **200**, 340–344 (1995)
28. Ionicioiu, R., Zanardi, P., Rossi, F.: Testing Bell's inequality with ballistic electrons in semiconductors. Phys. Rev. A **63**, 050,101(R) (2001)
29. Jakóbczyk, L., Jamróz, A.: Entanglement and nonlocality versus spontaneous emission in two-atom systems. Phys. Lett. A **318**, 318–326 (2003)
30. Jakóbczyk, L., Jamróz, A.: Noise-induced finite-time disentanglement in two-atomic system. Phys. Lett. A **333**, 35–45 (2004)
31. Jamróz, A.: Local aspects of disentanglement induced by spontaneous emission. J. Phys. A **39**, 7727–7735 (2006)
32. Kofman, A.G., Korotkov, A.N.: Analysis of Bell inequality violation in superconducting phase qubits. Phys. Rev. B **77**, 104,502 (2008)
33. Kofman, A.G., Korotkov, A.N.: Bell-inequality violation versus entanglement in the presence of local decoherence. Phys. Rev. A **77**, 052,329 (2008)
34. Kofman, A.G., Zhang, Q., Martinis, J.M., Korotkov, A.N.: Theoretical analysis of measurement crosstalk for coupled Josephson phase qubits. Phys. Rev. B **75**, 014,524 (2007)
35. Li, S.B., Xu, J.B.: Entanglement, Bell violation, and phase decoherence of two atoms inside an optical cavity. Phys. Rev. A **72**, 022,332 (2005)
36. Ling, A., Peloso, M.P., Marcikic, I., Scarani, V., Lamas-Linares, A., Kurtsiefer, C.: Experimental quantum key distribution based on a Bell test. Phys. Rev. A **78**, 020,301 (2008)
37. Martinis, J.M., Nam, S., Aumentado, J., Urbina, C.: Rabi oscillations in a large Josephson-junction qubit. Phys. Rev. Lett. **89**, 117,901 (2002)
38. Matsukevich, D.N., Maunz, P., Moehring, D.L., Olmschenk, S., Monroe, C.: Bell inequality violation with two remote atomic qubits. Phys. Rev. Lett. **100**, 150,404 (2008)
39. McDermott, R., Simmonds, R.W., Steffen, M., Cooper, K.B., Cicak, K., Osborn, K.D., Oh, S., Pappas, D.P., Martinis, J.M.: Simultaneous state measurement of coupled Josephson phase qubits. Science **307**, 1299–1302 (2005)
40. Milburn, G.J.: Intrinsic decoherence in quantum mechanics. Phys. Rev. A **44**, 5401–5406 (1991)
41. Moehring, D.L., Madsen, M.J., Blinov, B.B., Monroe, C.: Experimental Bell inequality violation with an atom and a photon. Phys. Rev. Lett. **93**, 090,410 (2004)
42. Nielsen, M.A., Chuang, I.L.: Quantum Computation and Quantum Information. Cambridge University Press, Cambridge (2000)

43. Popescu, S., Rohrlich, D.: Generic quantum nonlocality. Phys. Lett. A **166**, 293–297 (1992)
44. Popescu, S., Rohrlich, D.: Which states violate Bell's-inequality maximally. Phys. Lett. A **169**, 411–414 (1992)
45. Rowe, M.A., Kielpinski, D., Meyer, V., Sackett, C.A., Itano, W.M., Monroe, C., Wineland, D.J.: Experimental violation of a Bell's inequality with efficient detection. Nature **409**, 791–794 (2001)
46. Samuelsson, P., Buttiker, M.: Dynamic generation of orbital quasiparticle entanglement in mesoscopic conductors. Phys. Rev. B **71**, 245,317 (2005)
47. Samuelsson, P., Sukhorukov, E.V., Büttiker, M.: Orbital entanglement and violation of Bell inequalities in mesoscopic conductors. Phys. Rev. Lett. **91**, 157,002 (2003)
48. Santos, M.F., Milman, P., Davidovich, L., Zagury, N.: Direct measurement of finite-time disentanglement induced by a reservoir. Phys. Rev. A **73**, 040,305(R) (2006)
49. Schlienz, J., Mahler, G.: Description of entanglement. Phys. Rev. A **52**, 4396–4404 (1995)
50. Schrödinger, E.: Discussion of probability relations between separated systems. Proc. Camb. Phil. Soc. **31**, 555–563 (1935)
51. Steffen, M., Ansmann, M., Bialczak, R.C., Katz, N., Lucero, E., McDermott, R., Neeley, M., Weig, E.M., Cleland, A.N., Martinis, J.M.: Measurement of the entanglement of two superconducting qubits via state tomography. Science **313**, 1423–1425 (2006)
52. Tolkunov, D., Privman, V., Aravind, P.K.: Decoherence of a measure of entanglement. Phys. Rev. A **71**, 060,308(R) (2005)
53. Trauzettel, B., Jordan, A.N., Beenakker, C.W.J., Buttiker, M.: Parity meter for charge qubits: an efficient quantum entangler. Phys. Rev. B **73**, 235,331 (2006)
54. van Velsen, J.L., Kindermann, M., Beenakker, C.W.J.: Dephasing of entangled electron-hole pairs in a degenerate electron gas. Turk. J. Phys. **27**, 323–330 (2003)
55. Verstraete, F., Wolf, M.M.: Entanglement versus Bell violations and their behavior under local filtering operations. Phys. Rev. Lett. **89**, 170,401 (2002)
56. Vollbrecht, K.G.H., Werner, R.F.: Why two qubits are special. J. Math. Phys. **41**, 6772–6782 (2000)
57. Wei, L.F., xi Liu, Y., Nori, F.: Testing Bell's inequality in a constantly coupled Josephson circuit by effective single-qubit operations. Phys. Rev. B **72**, 104,516 (2005)
58. Wei, L.F., xi Liu, Y., Storcz, M.J., Nori, F.: Macroscopic Einstein–Podolsky–Rosen pairs in superconducting circuits. Phys. Rev. A **73**, 052,307 (2006)
59. Weihs, G., Jennewein, T., Simon, C., Weinfurter, H., Zeilinger, A.: Violation of Bell's inequality under strict Einstein locality conditions. Phys. Rev. Lett. **81**, 5039–5043 (1998)
60. Werner, R.F.: Quantum states with Einstein–Podolsky–Rosen correlations admitting a hidden-variable model. Phys. Rev. A **40**, 4277–4281 (1989)
61. Yu, T., Eberly, J.H.: Finite-time disentanglement via spontaneous emission. Phys. Rev. Lett. **93**, 140,404 (2004)
62. Yu, T., Eberly, J.H.: Quantum open system theory: bipartite aspects. Phys. Rev. Lett. **97**, 140,403 (2006)
63. Yu, Y., Han, S., Chu, X., Chu, S.I., Wang, Z.: Coherent temporal oscillations of macroscopic quantum states in a Josephson junction. Science **296**, 889–892 (2002)